Semiconductor Physics, Quantum Electronics & Optoelectronics, 2014. V. 17, N 2. P. 109-129.

PACS 72.10.Bg, 73.21.Cd, 73.50.Mx, 73.63.Hs

Theory of relaxation for spontaneous emission of Bloch oscillation radiation

V.N. Sokolov[1] and G.J. Iafrate[2]
[1]*V. Lashkaryov Institute of Semiconductor Physics, NAS of Ukraine,*
41, prospect Nauky, 03028 Kyiv, Ukraine
Phone: 38(044) 525-6175; fax: 525-6033; e-mail: sokolov@isp.kiev.ua
[2]*Department of Electrical and Computer Engineering,*
North Carolina State University, Raleigh, NC 27695-8617, USA
Phone: 1(919) 513-2310; fax: 513-1247; e-mail: gjiafrate@ncsu.edu

Abstract. A theory for the spontaneous emission (SE) of radiation for a Bloch electron traversing a single energy miniband of a superlattice (SL) in a cavity while undergoing scattering is presented. The Bloch electron is accelerated under the influence of superimposed constant external and internal inhomogeneous electric fields while radiating into a microcavity. The constant external electric field strength is chosen so that the emitted radiation lies in the terahertz spectral range. The quantum dynamics for the inhomogeneous field correction is obtained from a Wigner–Weisskopf-like long-time, time-dependent perturbation theory analysis based on the instantaneous eigenstates of the electric field-dependent Bloch Hamiltonian. It is shown that SE for the cavity-enhanced Bloch electron probability amplitude becomes damped and frequency shifted due to the perturbing inhomogeneity. The developed general quantum approach is applied to the case of elastic electron scattering due to SL interface roughness (SLIR). In the analysis, the interface roughness effects are separated into contributions from independent planar and cross-correlated neighboring planar interfaces; it is estimated that the cross-correlated contribution to the SE relaxation rate is relatively small compared to the independent planar contribution. When analyzing the total emission power, it is shown that the degradation effects from SLIR can be more than compensated for by the enhancements derived from microcavity-based confinement tuning.

Keywords: Bloch oscillations, spontaneous emission, semiconductor superlattices.

Manuscript received 03.02.14; revised version received 16.04.14; accepted for publication 12.06.14; published online 30.06.14.

1. Introduction

It has been known that spontaneous emission (SE) of photons from an optically active medium can be strongly enhanced or inhibited by controllably modifying the dielectric environment in which the emission of photons occurs [1, 2]. Relevant to the subject of this paper is the coherent emission of electromagnetic radiation from Bloch oscillations in electrically biased semiconductor superlattices (SLs) [3-12]. In the case when the bias is chosen that the radiation output is in the terahertz regime, this allows for the possibility of inversionless terahertz lasers [13].

A theory of microcavity-enhanced spontaneous emission (MESE) for a Bloch electron traversing a single energy band without scattering accelerating in an external constant electric field has recently been examined by the authors [14, 15]. The theoretical analysis was fully quantum mechanical in that the quantized radiation field was described in terms of the dominant rectangular microcavity waveguide mode in the Coulomb gauge; also the instantaneous eigenstates of the Bloch Hamiltonian were utilized as the basis states in describing the Bloch electron dynamics to all orders in the constant electric field. Analysis of the probability amplitudes, over integral multiples of the Bloch period,

resulted in selection rules for photon emission in both photon frequency and wave vector, showing preferable transitions to the Wannier–Stark ladder levels. It was shown that the SE rate could be enhanced over free space emission [16] by tuning the emission frequency to align with the cavity mode spectral density peak, thus resulting in an output power of several microwatts in the terahertz spectral range for a GaAs-based superlattice (SL) imbedded in a microcavity.

In this paper, we generalize the analysis of MESE for a Bloch electron accelerating through a single miniband of a SL structure to include the electron scattering. As an example, the additional interaction of the electron with a perturbing inhomogeneous electric field arising from interface roughness [17-19] inherent from the SL material process is studied. The intent in studying the effect of such a perturbing inhomogeneity is to determine its role in limiting the MESE process as a scattering influence that dephases the coherency of the Bloch oscillation, and to quantitatively determine how the MESE selection rules are influenced by such a perturbation. The theoretical approach developed herein is quite general and allows for the inclusion of electron-phonon scattering as well. In this work, however, SLs are only considered for which the miniband width is less than the LO-phonon energy thereby relaxing the need to consider phonon effects in this analysis. A host of other possible deleterious scattering mechanisms are discussed in the literature [7, 17-20]. The developed theoretical methods and details of derivations, which are not reflected in a reduced version [21] are fully described.

The paper is organized as follows. In Sec. II, the quantum approach is briefly reviewed, and the Hamiltonian for a Bloch electron in the quantum electrodynamic field of interest is developed. The classical external electric field is described in the vector potential gauge, and the quantized electromagnetic radiation field is described by the dominant microcavity TE_{10} rectangular waveguide mode in the Coulomb gauge; the general inhomogeneous electric field is treated in the scalar potential gauge. In neglecting the higher-order quantum field-field interaction term, it is shown that the total Hamiltonian for this problem reduces to the sum of three contributions, the Hamiltonian for the Bloch electron in the classical external electric field interacting with the inhomogeneity, the Hamiltonian of the free quantized electromagnetic field, and the Hamiltonian for the first-order interaction between the cavity quantum field and the accelerated Bloch electron. Further, the instantaneous eigenstates of the Bloch Hamiltonian and the states of the free radiation field are utilized as basis states in describing the time development, and in calculating the *one photon* SE transition rates of the accelerated Bloch electrons under the simultaneous perturbing action of the quantum cavity radiation field and the inhomogeneous potential energy. In Sec. III, the overall probability amplitude analysis for one photon emission is developed; as a result of treating the perturbing inhomogeneity in *long-time*, time-dependent perturbation theory relative to the Bloch-accelerated system in the electrodynamic radiation field, it is found that the SE amplitude for the cavity-enhanced Bloch electron radiation becomes damped and frequency shifted in the off-diagonal and diagonal matrix elements of the inhomogeneous potential energy with respect to the instantaneous Bloch eigenstates. This resulting SE amplitude for the cavity-enhanced Bloch radiation is strikingly reminiscent to the form obtained for the Boltzmann transport equation to describe scattering in the well-known relaxation-time approximation. Therefore, in Sec. IV, for purposes of showing trends with regard to simple Bloch oscillation dephasing effects as the electron undergoes scattering, the dephasing analysis is carried out for a *heuristic* constant relaxation-time approximation, where the damping term is assumed constant and the frequency shift is constant, in particular, zero. Also, since our basic quantum analysis excludes the dissipative effect of the cavity radiation field interacting with lossy cavity walls, use is made of a well-known phenomenological treatment of dissipation whereby the singular part of the density of states is replaced by a Lorentzian with a broadening parameter dependent on the quality factor of the microcavity. In analyzing the total power in this approximation, it is shown that the degradation effects from SLIR can be more than compensated for by the enhancements derived by microcavity-based confinement tuning. In Sec. V, the theoretical analysis is extended beyond the heuristic relaxation-time approximation and is developed for the specific case where the inhomogeneous potential energy is represented by a lattice comb of planar interface inhomogeneities of variable potential strength, where the SL planar interface roughness is characterized statistically by an ensemble averaged over the variable potential strength. It is found that both the frequency shift and the damping constant are dependent on the Brillouin zone vector component perpendicular to the SL direction, the characteristic correlation lengths, and the applied electric field. Further, since the required matrix elements for the inhomogeneous potential energy are separable in terms of planar and cross-planar interface roughness contributions, detailed analysis revealed that the cross-planar contribution to the SE relaxation rate is relatively small, representing less than roughly 10% of the total relaxation rate relative to the dominant independent planar contribution. In Sec. VI, a summary and discussion of overall results is given. The Appendix provides the details of the time-dependent double perturbation theory analysis used to calculate the probability amplitude.

2. Quantum approach: Dynamics based on instantaneous eigenstates

Dynamical properties are considered for the situation in which the electron is confined to a single miniband n_0 of SL with energy $\varepsilon_{n_0}(\mathbf{K})$, while the effects of interband

coupling are ignored [22, 23]. Therefore, the quantum dynamics is described by the time-dependent Schrödinger equation

$$i\hbar\partial |\Psi_{n_0}(\mathbf{r},t)\rangle/\partial t = H|\Psi_{n_0}(\mathbf{r},t)\rangle,$$

where the exact Hamiltonian

$$H = [\mathbf{p} - (e/c)\mathbf{A}]^2/2m_0 + V_c(\mathbf{r}) + H_r + V(\mathbf{r},t)$$

can be reduced to a sum of the following separate Hamiltonians

$$H = H_0 + V(\mathbf{r},t) + H_r + H_I .$$

Here, the first two terms represent the Hamiltonian, $H_0(t) = [\mathbf{p} + \mathbf{p}_c(t)]^2/2m_0 + V_c(\mathbf{r})$, for single electron in a periodic crystal potential, $V_c(\mathbf{r})$, interacting with a homogeneous electric field **E**, and the potential energy, $V(\mathbf{r},t)$, for the inhomogeneous electric field due to the impurities or interface roughness; although the special case for the scattering potential considered in this work is time independent, the developed general treatment is applicable to a general time-dependent perturbation $V(\mathbf{r},t)$. Also H_r is the Hamiltonian for the cavity mode electromagnetic radiation field (m_0 is the free-electron mass, c is the velocity of light in vacuum, and e is the electron charge). The total vector potential in the exact Hamiltonian consists of $\mathbf{A} = \mathbf{A}_c + \mathbf{A}_r$, where $\mathbf{A}_c = -(c/e)\mathbf{p}_c$ describes the external electric field with $\mathbf{p}_c(t) = e\int_{t_0}^{t}\mathbf{E}(t')dt' = e\mathbf{E}\,t$ for the time-independent homogeneous electric field turned on at initial time $t_0 = 0$; $\mathbf{A}_r$ describes the TE_{10} cavity mode of the quantized radiation field $\mathbf{E}_r$ with the frequency ω_q given by [24]

$$A_{r,y} = \sum_{q_z}\sqrt{\frac{4\pi\hbar c^2}{\omega_q \varepsilon V_0}}\sin(q_x x)\left(\hat{a}_q e^{iq_z z} + \hat{a}_q^{\dagger} e^{-iq_z z}\right), \quad (1)$$

and $A_{r,x} = A_{r,z} = 0$, where $\hat{a}_q^{\dagger}$ and $\hat{a}_q$ are the photon boson creation and annihilation operators, ε is the dielectric constant of the medium filling the waveguide of the length L_z and cross-section $L_x L_y$, $V_0 = L_x L_y L_z$, and $q_x = \pi/L_x$. For the chosen system geometry, the corresponding electric field $\mathbf{E}_r$ is polarized in the direction of the dc field, which is assumed to be oriented along the y axis (also the SL growth direction). The Hamiltonian for the quantized radiation field has the form $H_r = \sum_q \hbar\omega_q \hat{a}_q^{\dagger}\hat{a}_q$, where $\omega_q = \omega_c[1 + (q_z/q_x)^2]^{1/2}$ is the mode dispersion relation, and $\omega_c = q_x c/\sqrt{\varepsilon}$ is the angular cutoff frequency; also the guided mode wavelength is written as $\lambda = \lambda_c/[(\omega_q/\omega_c)^2 - 1]^{1/2}$, where $\lambda_c = 2L_x$ is the cutoff wavelength [25]. The Hamiltonian $H_I(t) = -(e/m_0 c)\mathbf{A}_r \cdot [\mathbf{p} + \mathbf{p}_c(t)]$, for the first-order interaction between the quantum field and the Bloch electron, couples both subsystems H_0 and H_r, and causes transitions between the accelerated Bloch electron states through photon absorption and emission. Then, starting with the reduced Hamiltonian $H = H_0 + H_r + H_I + V(\mathbf{r},t)$, use is made of first-order, *early-time* time-dependent perturbation theory [26, 27] to calculate SE transition probabilities between states of $H_0 + H_r$ while regarding $H_I(t) \sim \mathbf{A}_r \cdot [\mathbf{p} + \mathbf{p}_c(t)]$ as a perturbation, and at the *same* time, use is made of a *long-time* Wigner-Weisskopf approximate perturbation theory analysis [27, 28] to calculate the relaxation influence of $V(\mathbf{r},t)$ on the SE transition probabilities; this time scale ordering is invoked since SE rates are orders of magnitude faster than relaxation times due to $V(\mathbf{r},t)$.

The solution for $|\Psi_{n_0}(\mathbf{r},t)\rangle$ can be represented in terms of the eigenstates of basis states $|\psi_{n_0\mathbf{K}}(\mathbf{r},t),\{n_{\mathbf{q},j}\}\rangle = |\psi_{n_0\mathbf{K}}(\mathbf{r},t)\rangle|\{n_{\mathbf{q},j}\}\rangle$ of the unperturbed Hamiltonian $H_0 + H_r$ as

$$|\Psi_{n_0}(\mathbf{r},t)\rangle = \sum_{\mathbf{K}}\sum_{\{n_{\mathbf{q},j}\}} A_{\{n_{\mathbf{q},j}\}}(\mathbf{K},t)\,|\Psi_{n_0\mathbf{K}}(\mathbf{r},t),\{n_{\mathbf{q},j}\}\rangle\times$$

$$\times\exp\left\{-\frac{i}{\hbar}\int_{t_0}^{t}[\varepsilon_{n_0}(\mathbf{k}(t')) + \sum_{\mathbf{q},j}\hbar\omega_q n_{\mathbf{q},j}]dt'\right\}. \quad (2)$$

Here, the summation over $\mathbf{K}$ is carried out over the entire Brillouin zone, and $\{n_{\mathbf{q},j}\}$ is specified over all possible combinations of photon occupation number, $n_{\mathbf{q},j}$, with photon wave vector $\mathbf{q}$ and polarization $\hat{\varepsilon}_{\mathbf{q},j}$, $j = 1,2$. The instantaneous eigenstates of H_0 are given [22, 23] by $\psi_{n_0\mathbf{K}}(\mathbf{r},t) = \Omega^{-1/2}e^{i\mathbf{K}\cdot\mathbf{r}}u_{n_0\mathbf{k}(t)}(\mathbf{r})$, where $u_{n_0\mathbf{k}(t)}(\mathbf{r})$ is the periodic part of the Bloch function, $\mathbf{k}(t) = \mathbf{K} + \mathbf{p}_c(t)/\hbar$, and the values of the electron wave vector $\mathbf{K}$ are determined by the periodic boundary conditions of the periodic crystal of volume Ω.

For the case of *one photon* SE, which assumes that, initially, no photons are present in the radiation field, the probability amplitude in the wave function of Eq. (2) satisfies the initial condition $A_{\{n_{\mathbf{q},j}\}}(\mathbf{K},t_0) = \{\delta_{n_{\mathbf{q},j},0}\}\delta_{\mathbf{K},\mathbf{K}_0}$ at time $t = t_0$, when the electric field is turned on. Here, $\mathbf{K}_0$ and $n^0_{\mathbf{q},j} = 0$ are the initial values of $\mathbf{K}$ and $n_{\mathbf{q},j}$. The probability amplitude for SE, $A_{\{n_{\mathbf{q},j}\}}(\mathbf{K},t)$, is evaluated by double perturbation theory in the Appendix.

3. Probability amplitude analysis

A. Probability amplitudes – one photon emission

The appropriate time-dependent equations of motion for the $A_{\{n_{\mathbf{q},j}\}}(\mathbf{K},t)$ coefficients expressed in Eq. (2) relate the time rate of change of $A_{\{n_{\mathbf{q},j}\}}(\mathbf{K},t)$ to the basis-dependent matrix elements of H_I and $V(\mathbf{r},t)$ through a self-consistent set of equations. In applying *early-time*, first-order perturbation theory to the H_I-coefficients of the set of equations, and applying a *long-time*, Wigner–Weisskopf-like approximation to the V-coefficients of the set of equations, we obtain [see Appendix, Eq. (A12)] a closed form of inhomogeneous equation for the one photon SE amplitude

$$\dot{A}_n(\mathbf{K}_0,t)-\frac{1}{i\hbar}f_{\mathbf{K}_0\mathbf{K}_0}(t)A_n(\mathbf{K}_0,t)+$$
$$+\frac{1}{\hbar^2}\int_0^t dt'\sum_{\mathbf{K}'\neq\mathbf{K}_0}f_{\mathbf{K}_0\mathbf{K}'}(t)f^*_{\mathbf{K}_0\mathbf{K}'}(t')A_n(\mathbf{K}_0,t')=$$
$$=\dot{A}^0_q(\mathbf{K}_0,t)+\frac{1}{i\hbar}\sum_{\mathbf{K}'\neq\mathbf{K}_0}f_{\mathbf{K}_0,\mathbf{K}'}(t)\,A^0_q(\mathbf{K}',t)\,. \qquad (3)$$

Here, $t_0=0$, $\{n_{\mathbf{q},j}\}\to n=1$, $\mathbf{k}_0(t)=\mathbf{K}_0+\mathbf{p}_c(t)/\hbar$, and

$$f_{\mathbf{K}_0\mathbf{K}'}(t)=V_{\mathbf{K}_0\mathbf{K}'}(t)\exp\left\{\frac{i}{\hbar}\int_0^t\{\varepsilon_{n_0}[\mathbf{k}_0(t')]-\varepsilon_{n_0}[\mathbf{k}'(t')]\}\,dt'\right\}, \qquad (4)$$

where $V_{\mathbf{K}_0\mathbf{K}'}(t)=\left(\psi_{n_0\mathbf{K}_0}(\mathbf{r},t),V(\mathbf{r},t)\psi_{n_0\mathbf{K}'}(\mathbf{r},t)\right)$ are the appropriate matrix elements of the perturbing inhomogeneity, $V(\mathbf{r},t)$; the general time dependence of the matrix elements originates from both the explicit time dependence of $V(\mathbf{r},t)$ and from the time dependence of $\mathbf{k}(t)=\mathbf{K}+\mathbf{p}_c(t)/\hbar$. Also,

$$A^0_q(\mathbf{K}_0,t)=D(q_x/q)^{1/2}\int_0^t dt' v_y[\mathbf{k}_0(t')-\mathbf{q}_s]\times$$
$$\times\exp\left\{-\frac{i}{\hbar}\int_0^{t'}\{\varepsilon_{n_0}[\mathbf{k}_0(t_1)]-\varepsilon_{n_0}[\mathbf{k}_0(t_1)-\mathbf{q}_s]-\hbar\omega_q\}\,dt_1\right\}, \qquad (5)$$

the probability amplitude for the microcavity-based SE alone [14]; $D=-i\sqrt{\pi c\alpha/\omega_c\varepsilon V_0}$, $\alpha=e^2/\hbar c$ is the fine structure constant, $\mathbf{q}_s=\{\pm q_x,0,q_z\}$ with "+" for $s=1$ and "–" for $s=2$, $q=(q_x^2+q_z^2)^{1/2}$, and $v_y[\mathbf{k}(t)]=(1/\hbar)\nabla_{K_y}\varepsilon_{n_0}(\mathbf{K})|_{\mathbf{k}(t)}$, the y component of Bloch velocity in the band.

B. Analysis of one photon SE amplitude equation

The solution for $A_n(\mathbf{K}_0,t)$ in Eq. (3) depends explicitly on $f_{\mathbf{K}_0\mathbf{K}'}(t)$ as noted in Eq. (4). The time dependence of $f_{\mathbf{K}_0\mathbf{K}'}(t)$, expressed through the time-dependent matrix elements of $V(\mathbf{r},t)$ and through the time dependence of accelerated instantaneous energy eigenstates in the phase of $f_{\mathbf{K}_0\mathbf{K}'}(t)$, are now addressed. For the type of potential energy function of interest in this problem, that is, one where $V(\mathbf{r},t)\equiv V(\mathbf{r})$, a function of position alone, and where $V(\mathbf{r})$ is *a comb of abruptly changing, planar, interface inhomogeneities positioned at the SL lattice sites with randomly distributed planar interface roughness*, one can find the analytic solution to Eq. (3) quite readily. Attention is now focused on the closed form inhomogeneous equation for the one photon SE amplitude noted in Eq. (3).

1. The potential energy consideration

In the Wannier representation, the instantaneous eigenstates, $\psi_{n_0\mathbf{K}}(\mathbf{r},t)$, are equivalently expressed as

$$\psi_{n_0\mathbf{K}}(\mathbf{r},t)=\frac{1}{N_0^{1/2}}e^{-i\frac{\mathbf{p}_c(t)}{\hbar}\cdot\mathbf{r}}\sum_{\mathbf{l}}e^{i\left(\mathbf{K}+\mathbf{p}_c(t)/\hbar\right)\cdot\mathbf{l}}W_{n_0}(\mathbf{r}-\mathbf{l}), \qquad (6)$$

where $N_0=N_yN_\perp$ is the total number of lattice sites, and $W_{n_0}(\mathbf{r}-\mathbf{l})$ are the Wannier functions, which are independent of $\mathbf{K}$ [29], defined over all the lattice sites, $\mathbf{l}$, of a given band, n_0. Then, in taking the matrix elements of $V(\mathbf{r})$ with $\psi_{n_0\mathbf{K}}(\mathbf{r},t)$ in Eq. (6), one obtains

$$V_{\mathbf{K}\mathbf{K}'}(t)=\frac{1}{N_0}\sum_{\mathbf{l},\mathbf{l}'}e^{i(\mathbf{K}'\cdot\mathbf{l}'-\mathbf{K}\cdot\mathbf{l})}V_{\mathbf{l}\mathbf{l}'}e^{i\frac{\mathbf{p}_c(t)}{\hbar}\cdot(\mathbf{l}'-\mathbf{l})}, \qquad (7)$$

where $V_{\mathbf{l}\mathbf{l}'}=\int d\mathbf{r}\,W^*_{n_0}(\mathbf{r}-\mathbf{l})V(\mathbf{r})W_{n_0}(\mathbf{r}-\mathbf{l}')$. The matrix elements in Eq. (7) are seen to be dependent on time through the $\mathbf{p}_c(t)$ dependence or, equivalently, through $\mathbf{k}(t)=\mathbf{K}+\mathbf{p}_c(t)/\hbar$.

For the case where $V(\mathbf{r})$ is a lattice comb of planar interface inhomogeneities with randomly distributed planar interface roughness, $V_{\mathbf{l}\mathbf{l}'}$ can be expressed as $V_{\mathbf{l}\mathbf{l}'}=\sum_{\mathbf{l}_r}v(\mathbf{l}_r)\delta_{\mathbf{l}\mathbf{l}_r}\delta_{\mathbf{l}'\mathbf{l}_r}$, so that

$$V_{\mathbf{K}\mathbf{K}'}=\frac{1}{N_0}\sum_{\mathbf{l}_r}v(\mathbf{l}_r)\,e^{i(\mathbf{K}'-\mathbf{K})\cdot\mathbf{l}_r}. \qquad (8)$$

Here, $v(\mathbf{l}_r)$ includes the effect of the SL interface roughness which is generally accounted for [30] independent planar interfaces by an ensemble averaged autocorrelation function in the form

$$\langle v(\mathbf{l}_r)v^*(\mathbf{l}'_r)\rangle=\delta_{l_{ry}l'_{ry}}\langle|v(l_{ry})|^2\rangle\,e^{-(\mathbf{l}_{r\perp}-\mathbf{l}'_{r\perp})^2/\Lambda_y^2} \qquad (9)$$

and

$$\langle v(\mathbf{l}_r)\rangle=0, \qquad (10)$$

with $\mathbf{l}_r = \{l_{ry}, \mathbf{l}_{r\perp}\}$. Later, we consider the effect of SL interface roughness from cross-correlated neighboring planar interfaces. It is noted that an equivalent abrupt interface model has been utilized in Refs. [31, 32] based on potential with similar correlation properties. The Fourier transform of the autocorrelation function is a specific Gaussian [33] assumption with two parameters which characterize the rms height of the interface potential fluctuations and the roughness correlation length. Other forms may be more suitable [34] based on empirical data.

2. The evaluation of the integral of the instantaneous eigenstates

Since $V_{\mathbf{KK}'}$ is time independent, for the potential energy of interest, the only other source of time dependence in $f_{\mathbf{KK}'}(t)$ comes from the accelerated instantaneous energy eigenstates, $\varepsilon_{n_0}[\mathbf{k}(t)]$, in the phase of $f_{\mathbf{KK}'}(t)$ in Eq. (4). This time dependence in a constant electric field can be expressed as

$$I_{n_0} \equiv \int_0^t \varepsilon_{n_0}[\mathbf{K} + \mathbf{p}_c(t')/\hbar]\, dt' = \\ = \bar{\varepsilon}_{n_0}(\mathbf{K}_\perp)t + i\eta(\mathbf{K},0) - i\eta(\mathbf{K},t), \tag{11}$$

where

$$\bar{\varepsilon}_{n_0}(\mathbf{K}_\perp) = \frac{1}{N_y}\sum_{K_y} \varepsilon_{n_0}(K_y, \mathbf{K}_\perp); \tag{12}$$

and

$$\eta(\mathbf{K},t) = \sum_{\ell_y \neq 0} \frac{\varepsilon_{n_0}(a\ell_y, \mathbf{K}_\perp)}{\omega_B \ell_y} e^{i(K_y a + \omega_B t)\ell_y} \tag{13}$$

with

$$\varepsilon_{n_0}(a\ell_y, \mathbf{K}_\perp) = \frac{1}{N_y}\sum_{K_y} \varepsilon_{n_0}(K_y, \mathbf{K}_\perp) e^{-iK_y a\ell_y}, \tag{14}$$

$\omega_B = eEa/\hbar$ the Bloch frequency, a the SL period, and ℓ_y an integer. In (12), $\bar{\varepsilon}_{n_0}(\mathbf{K}_\perp) \equiv \overline{\varepsilon_{n_0}(\mathbf{K})}$ is the average value of $\varepsilon_{n_0}(\mathbf{K})$ along the K_y direction in the Brillouin zone, dependent on $\mathbf{K}_\perp$ alone. In particular, in (13), when the nearest-neighbor tight-binding (NNTB) approximation is considered, only the terms with $\ell_y = \pm 1$ need be retained in the sum.

In order to arrive at the result of Eq. (11), we develop the time integral required by expressing $\varepsilon_{n_0}(\mathbf{K})$ in the Wannier representation. As such, $\varepsilon_{n_0}(\mathbf{K})$ can be written as

$$\varepsilon_{n_0}(\mathbf{K}) = \sum_{\mathbf{l}} \varepsilon_{n_0}(\mathbf{l}) e^{i\mathbf{K}\cdot\mathbf{l}}, \tag{15}$$

where

$$\varepsilon_{n_0}(\mathbf{l}) = \frac{1}{N_0}\sum_{\mathbf{K}} \varepsilon_{n_0}(\mathbf{K}) e^{-i\mathbf{K}\cdot\mathbf{l}}. \tag{16}$$

Then, it follows that, for a constant electric field, with $\mathbf{p}_c \cdot \mathbf{l} = \hbar\omega_B \ell_y t$, the phase integral, I_{n_0}, becomes

$$I_{n_0} = \sum_{\mathbf{l}} \varepsilon_{n_0}(\mathbf{l})\, e^{i\mathbf{K}\cdot\mathbf{l}} \frac{e^{i\omega_B \ell_y t} - 1}{i\omega_B \ell_y}. \tag{17}$$

Equation (17) can be rewritten explicitly in terms of $\ell_y = 0$ and $\ell_y \neq 0$ contributions, which when using Eq. (16) results in

$$I_{n_0} = \bar{\varepsilon}_{n_0}(\mathbf{K}_\perp)t + \sum_{\ell_y \neq 0} \varepsilon_{n_0}(a\ell_y, \mathbf{K}_\perp)\, e^{iK_y a\ell_y} \frac{e^{i\omega_B \ell_y t} - 1}{i\,\omega_B \ell_y}. \tag{18}$$

Here, $\bar{\varepsilon}_{n_0}(\mathbf{K}_\perp)$ is given in (12) and $\varepsilon_{n_0}(a\ell_y, \mathbf{K}_\perp)$ is given in (14), which gives the result of Eq. (11). In further considering the integral, I_{n_0}, in Eq. (11), but instead over the limits from 0 to t, the same procedure is followed, but with limits from t' to t, to obtain

$$\int_{t'}^{t} \varepsilon_{n_0}[\mathbf{K} + \mathbf{p}_c(t'')/\hbar]\, dt'' = \\ = \bar{\varepsilon}_{n_0}(\mathbf{K}_\perp)(t - t') + i\eta(\mathbf{K},t') - i\eta(\mathbf{K},t), \tag{19}$$

where $\eta(\mathbf{K},t)$ is given by Eq. (13).

The variables defined by Eqs. (12), (13), and (14) are central to the entire analysis. Although they are formally defined for a general band structure, they are evaluated here for the *specific SL miniband dispersion relation* expressed as

$$\varepsilon_{n_0}(\mathbf{K}) = \varepsilon_{n_0}(0) + \sum_{l'=1}^{\infty} \Delta_{l'} \sin^2 \frac{l' a K_y}{2} + \varepsilon_\perp(\mathbf{K}_\perp), \tag{20}$$

where $\varepsilon_{n_0}(0)$ is the miniband edge, $\Delta_{l'}$ is the width of the l'-th miniband harmonic of SL, and $\varepsilon_\perp(\mathbf{K}_\perp)$ is the contribution from the perpendicular components of the band. Such a form for the energy band dispersion in the SL growth direction generally includes long range coupling over the neighboring quantum wells (QWs) with a relative strength measured by the specific value of the ratio $\Delta_{l'+1}/\Delta_{l'} < 1$, which is strongly dependent on the extent of wave function overlap. In putting the expression for $\varepsilon_{n_0}(\mathbf{K})$ from Eq. (20) into Eq. (12) and using $\sum_{K_y}(\cdots) = \frac{N_y a}{2\pi}\int_{-\pi/a}^{\pi/a} dK_y(\cdots)$, one obtains

$$\bar{\varepsilon}_{n_0}(\mathbf{K}_\perp) = \varepsilon_{n_0}(0) + \sum_{l'=1}^{\infty} \frac{\Delta_{l'}}{2} + \varepsilon_\perp(\mathbf{K}_\perp). \tag{21}$$

Also, for $\varepsilon_{n_0}(a\ell_y, \mathbf{K}_\perp)$ in Eq. (14), one similarly obtains $\varepsilon_{n_0}(a\ell_y, \mathbf{K}_\perp) = -\frac{1}{2}\Delta_{|\ell_y|}$ and in using this expression in Eq. (13), $\eta(K) \equiv \eta(\mathbf{K},0)$ becomes

$$\eta(\mathbf{K}) = -i\sum_{\ell_y=1}^{\infty} \frac{\Delta_{\ell_y}}{2\omega_B \ell_y} \sin(K_y a \ell_y). \quad (22)$$

Therefore, for the assumed miniband dispersion, $\overline{\varepsilon_{n_0}(\mathbf{K})}$ depends only on $\mathbf{K}_\perp$, $\varepsilon_{n_0}(a\ell_y, \mathbf{K}_\perp)$ is constant, and $\eta(\mathbf{K})$ depends only on K_y.

The result of Eq. (11) is a significant reduction of I_{n_0} and allows one to develop a simple time-dependent expression for $f_{\mathbf{KK}'}(t)$ as

$$f_{\mathbf{KK}'}(t) = \\ = V_{\mathbf{KK}'} e^{\frac{1}{\hbar}\{[\eta(\mathbf{K},t)-\eta(\mathbf{K}',t)]-[\eta(\mathbf{K})-\eta(\mathbf{K}')]\}} e^{\frac{i}{\hbar}\left[\bar{\varepsilon}_{n_0}(\mathbf{K}_\perp)-\bar{\varepsilon}_{n_0}(\mathbf{K}'_\perp)\right]t}, \quad (23)$$

where $V_{\mathbf{KK}'}$ is given in Eq. (8), $\eta(\mathbf{K},t)$ is given in Eq. (13), and $\bar{\varepsilon}_{n_0}(\mathbf{K}_\perp)$ is given in Eq. (12).

3. Solution to SE amplitude equation for planar interface roughness

In looking for the solution to Eq. (3) for the potential energy function defined by matrix elements $V_{\mathbf{KK}'}$ given in Eq. (8), with $v(\mathbf{l})$ satisfying ensemble average values given in (9) and (10), it has been already shown that $f_{\mathbf{KK}'}(t)$ is given by Eq. (23); also, from (4), it follows that

$$f_{\mathbf{KK}'}(t) f^*_{\mathbf{KK}'}(t') = \\ = |V_{\mathbf{KK}'}|^2 \exp\left\{\frac{i}{\hbar}\int_{t'}^{t} [\varepsilon_{n_0}(\mathbf{K}+\mathbf{p}_c/\hbar) - \varepsilon_{n_0}(\mathbf{K}'+\mathbf{p}_c/\hbar)]\, dt''\right\}. \quad (24)$$

It then follows from the use of Eq. (19) in Eq. (24) that

$$f_{\mathbf{KK}'}(t) f^*_{\mathbf{KK}'}(t') = \gamma_{\mathbf{KK}'}(t,t') e^{i\omega_{\mathbf{KK}'}(t-t')} \quad (25)$$

with $\omega_{\mathbf{KK}'} = [\bar{\varepsilon}_{n_0}(\mathbf{K}_\perp) - \bar{\varepsilon}_{n_0}(\mathbf{K}'_\perp)]/\hbar$ and

$$\gamma_{\mathbf{KK}'}(t,t') = |V_{\mathbf{KK}'}|^2 e^{-\frac{1}{\hbar}\{[\eta(\mathbf{K},t')-\eta(\mathbf{K}',t')]-[\eta(\mathbf{K},t)-\eta(\mathbf{K}',t)]\}}, \quad (26)$$

where

$$|V_{\mathbf{KK}'}|^2 = \frac{1}{N_0^2}\sum_{\mathbf{l},\mathbf{l}'} v(\mathbf{l}) v^*(\mathbf{l}') e^{i(\mathbf{K}-\mathbf{K}')\cdot(\mathbf{l}-\mathbf{l}')}. \quad (27)$$

After ensemble averaging over the interface roughness, it is clear from Eqs. (9) and (10) that the diagonal matrix elements $V_{\mathbf{KK}} = (1/N_0)\sum_{\mathbf{l}} v(\mathbf{l})$ and the matrix elements in Eq. (8) ensemble average to zero because $\langle v(\mathbf{l})\rangle = 0$ at each $\mathbf{l}$; but $|V_{\mathbf{KK}'}|^2$ survives because Eq. (27) contains ensemble averages over $\langle v(\mathbf{l}) v^*(\mathbf{l}')\rangle$ which obeys an autocorrelation relation from Eq. (9).

Therefore, in putting $f_{\mathbf{KK}'}(t)$ and $f_{\mathbf{KK}'}(t) f^*_{\mathbf{KK}'}(t')$ into Eq. (3), and taking the ensemble average to lowest order (dropping the ensemble average symbol for mathematical convenience), one obtains the SE amplitude equation as

$$\dot{A}_n(\mathbf{K}_0,t) + \frac{i}{\hbar} V_{\mathbf{K}_0\mathbf{K}_0} A_n(\mathbf{K}_0,t) + \\ + \frac{1}{\hbar^2}\sum_{\mathbf{K}'\neq\mathbf{K}_0} \int_0^t dt' \gamma_{\mathbf{K}_0\mathbf{K}'}(t,t') e^{i\omega_{\mathbf{K}_0\mathbf{K}'}(t-t')} A_n(\mathbf{K}_0,t') = \quad (28) \\ = \dot{A}^0_q(\mathbf{K}_0,t).$$

Here, the ensemble average of $V_{\mathbf{K}_0\mathbf{K}_0}$ is zero, but we retain the diagonal element to show the systematic behavior of perturbation theory in what follows.

Equation (24) contains an integral form which requires the explicit time-dependent specification of $\gamma_{\mathbf{K}_0\mathbf{K}'}(t,t')$ defined through $\eta(K_y a + \omega_B t, \mathbf{K}_\perp)$ and $\eta(K_y a + \omega_B t', \mathbf{K}_\perp)$, where $\eta(\mathbf{K})$ is given in Eq. (22). For NNTB, in the SL band of interest, we see from Eq. (22) that $\eta(K_y a, \mathbf{K}_\perp) = -i\frac{\Delta_1}{2\omega_B}\sin(K_y a)$. Then $\gamma_{\mathbf{KK}'}(t,t')$ from Eq. (26) becomes

$$\gamma_{\mathbf{KK}'}(t,t') = \\ |V_{\mathbf{KK}'}|^2 e^{i\xi\{[\sin(K_y a+\omega_B t')-\sin(K'_y a+\omega_B t')]-[\sin(K_y a+\omega_B t)-\sin(K'_y a+\omega_B t)]\}}, \quad (29)$$

where $\xi = \Delta_1/2\hbar\omega_B$. In utilizing the well-known result [35] $\exp(i\xi\sin\alpha) = \sum_{m=-\infty}^{\infty} J_m(\xi)\exp(im\alpha)$, where $J_m(\xi)$ is the m-th order Bessel function of the first kind, it then follows that $\gamma_{\mathbf{KK}'}(t,t')$ can be expressed as a product of four sums over Bessel functions with differing indices, which when placed in (28) and ordered appropriately with respect to indices and time, results in the equation

$$\dot{A}_n(\mathbf{K}_0,t) + \frac{i}{\hbar} V_{\mathbf{K}_0\mathbf{K}_0} A_n(\mathbf{K}_0,t) + \frac{1}{\hbar^2}\sum_{\mathbf{K}'\neq\mathbf{K}_0} |V_{\mathbf{K}_0\mathbf{K}'}|^2 \times \\ \times \sum_{m,m'=-\infty}^{\infty} J_m(\xi) J_{m'}(\xi) e^{im(K_{0y}-K'_y)a} \times \\ \times \sum_{m'',m'''=-\infty}^{\infty} J_{m''}(\xi) J_{m'''}(\xi) e^{-im''(K_{0y}-K'_y)a} e^{iK'_y a[(m-m')-(m''-m''')]} \times \\ \times \int_0^t dt' e^{\frac{i}{\hbar}\left[\bar{\varepsilon}_{n_0}(\mathbf{K}_{0\perp})-\bar{\varepsilon}_{n_0}(\mathbf{K}'_\perp)\right](t-t')} \times \\ \times e^{-i\omega_B(m''-m''')(t-t')} e^{i\omega_B[(m-m')-(m''-m''')]t'} A_n(\mathbf{K}_0,t') \\ = \dot{A}^0_q(\mathbf{K}_0,t). \quad (30)$$

Eq. (30) is solved by Laplace transform, and an analytic solution can be obtained in the *long-time* limit. We note that the temporal integral in Eq. (30) is in the form appropriate to apply the convolution theorem. However, with $F_n(s)$ noted as the Laplace transform of $A_n(\mathbf{K}_0,t)$, the term $e^{i[(m-m')-(m''-m''')]\omega_B t'}A_n(\mathbf{K}_0,t')$ under the integral, which gives rise to the Laplace transform component $F_n\{s-i[(m-m')-(m''-m''')]\omega_B\}$, is rapidly oscillatory for $m-m'\neq m''-m'''$ as t' grows; thus, for $\omega_B t'>>1$, the terms in the four-fold sum for which $m-m'=m''-m'''$ dominate in the long-time limit. Therefore, the terms with $m-m'=m''-m'''$ only are retained in the four-fold sum while all other terms are neglected. Thus, in letting $F_n(s)=\int_0^\infty e^{-st}A_n(t)dt\equiv L\{A_n(t)\}$, Eq. (30) can be transformed to get

$$F_n(s)=\frac{A_n(\mathbf{K}_0,0)}{s+\frac{i}{\hbar}V_{\mathbf{K}_0\mathbf{K}_0}+i\Delta(s)}+\frac{L\{\dot{A}_q^0(\mathbf{K}_0,t)\}}{s+\frac{i}{\hbar}V_{\mathbf{K}_0\mathbf{K}_0}+i\Delta(s)}, \quad (31)$$

where

$$\Delta(s)=\frac{1}{\hbar^2}\sum_{m=-\infty}^{\infty}R_m\sum_{\mathbf{K}'_\perp\neq\mathbf{K}_{0\perp}}\frac{\left|V_{\mathbf{K}_0\mathbf{K}'}\right|^2}{(\omega_{K_0K'}-m\omega_B)+is}. \quad (32)$$

Also, $R_m(\xi)$ in Eq. (32) has its origin from summing over the term $\sum_{K'_y\neq K_{0y}}|G_{K_{0y}\neq K'_y}|^2\equiv R_m$ in Eq. (30), where

$$G_{K_{0y},K'_y}(\xi,m)=\sum_{m'=-\infty}^{\infty}J_{m'}(\xi)J_{m'-m}(\xi)\,e^{im'(K_{0y}-K'_y)a}.$$

We then find that

$$R_m(\xi)=N_y\sum_{m'=-\infty}^{\infty}J_{m'}^2(\xi)J_{m'+m}^2(\xi)-\delta_{m,0}; \quad (33)$$

hereafter we omit a comparatively small additional term, $\delta_{m,0}$, compared to the leading term which is proportional to N_y, the number of SL sites in the y direction. Then $A_n(\mathbf{K}_0,t)=L^{-1}\{F_n(s)\}$ is the inverse transform of (31) for all t. However, one can obtain the *long-time* behavior of $A_n(\mathbf{K}_0,t)$ by examining (31) in the limit $\Delta(s\to 0)$. In using the well-known relation $\lim_{s\to 0}\left[\frac{1}{x+is}\right]=P\left(\frac{1}{x}\right)-i\pi\delta(x)$, it is clear that

$$i\Delta(0)=\frac{i}{\hbar^2}\sum_{m=-\infty}^{\infty}R_m\sum_{\mathbf{K}'_\perp\neq\mathbf{K}_{0\perp}}\frac{|V_{\mathbf{K}_0\mathbf{K}'}|^2}{\omega_{\mathbf{K}_0\mathbf{K}'}-m\omega_B}+$$
$$+\frac{\pi}{\hbar^2}\sum_{m=-\infty}^{\infty}R_m\sum_{\mathbf{K}'_\perp\neq\mathbf{K}_{0\perp}}|V_{\mathbf{K}_0\mathbf{K}'}|^2\,\delta(\omega_{\mathbf{K}_0\mathbf{K}'}-m\omega_B). \quad (34)$$

Therefore, in the long-time limit, dropping the homogeneous solution and keeping the inhomogeneous solution in Eq. (31), we obtain

$$F_n(s)=\frac{L\{\dot{A}_q^0(\mathbf{K}_0,t)\}}{s+\frac{i}{\hbar}V_{\mathbf{K}_0\mathbf{K}_0}+i\Delta(0)}\equiv\frac{L\{\dot{A}_q^0(\mathbf{K}_0,t)\}}{s+i\Delta\omega(\mathbf{K}_0)+\frac{\Gamma(\mathbf{K}_0)}{2}}, \quad (35)$$

where

$$\hbar\Delta\omega(\mathbf{K}_0)=V_{\mathbf{K}_0\mathbf{K}_0}+$$
$$+\sum_{m=-\infty}^{\infty}R_m\sum_{\mathbf{K}'_\perp\neq\mathbf{K}_{0\perp}}\frac{|V_{\mathbf{K}_0\mathbf{K}'}|^2}{\bar{\varepsilon}_{n_0}(\mathbf{K}_{0\perp})-\bar{\varepsilon}_{n_0}(\mathbf{K}'_\perp)-m\hbar\omega_B}, \quad (36)$$

and

$$\Gamma(\mathbf{K}_0)=\frac{2\pi}{\hbar}\sum_{m=-\infty}^{\infty}R_m\sum_{\mathbf{K}'_\perp\neq\mathbf{K}_{0\perp}}|V_{\mathbf{K}_0\mathbf{K}'}|^2\times$$
$$\times\delta[\bar{\varepsilon}_{n_0}(\mathbf{K}_{0\perp})-\bar{\varepsilon}_{n_0}(\mathbf{K}'_\perp)-m\hbar\omega_B]. \quad (37)$$

The inverse Laplace transform of (35) is

$$A_n(\mathbf{K}_0,t)=\int_0^t dt'\,\dot{A}_q^0(\mathbf{K}_0,t')e^{-i\Delta\omega(\mathbf{K}_0)(t-t')}e^{-\frac{\Gamma(\mathbf{K}_0)}{2}(t-t')}. \quad (38)$$

$A_n(\mathbf{K}_0,t)$ in Eq. (38) is a key result and shows that the SE for the cavity-enhanced Bloch electron probability amplitude becomes damped by $\Gamma(\mathbf{K}_0)$ in Eq. (37) and frequency shifted by $\Delta\omega(\mathbf{K}_0)$ in Eq. (36) due to the perturbing influence of the constant external electric field and the assumed interface inhomogeneity. It is interesting to note that the result obtained in Eq. (38) is strikingly reminiscent of the result obtained for the Boltzmann transport equation to describe the scattering processes in the well-known relaxation-time approximation [36]. Therefore, in an approach similar to analyzing the complications of the Boltzmann theory, we first consider the model, noted here as the *constant relaxation-time approximation*, where $\Delta\omega(\mathbf{K}_0)$ is assumed to be a constant, chosen to be zero for convenience, and $\Gamma(\mathbf{K}_0)$ is assumed to be a constant, independent of wave vector $\mathbf{K}_0$, to analyze, in the simplest heuristic approximation, the dephasing effects due to interface roughness.

The frequency shift in Eq. (36) is essentially, to within R_m, the second-order perturbation correction for the inhomogeneity and the external field, and the energy difference in the denominator is taken with respect to the average value of the energy band in the direction of the constant electric field, which is the y direction. It is noted that the frequency shift can be expressed in terms of the Green function for the field-dependent SL Wannier functions in the NNTB approximation as [37]

$$G_0(\xi,l,l';\delta\varepsilon)=\sum_{m'=-\infty}^{\infty}\frac{J_{l+m'}(\xi)J_{l'+m'}(\xi)}{\delta\varepsilon-m'\hbar\omega_B}. \quad (39)$$

Then, $\hbar\Delta\omega(\mathbf{K}_0)$ in Eq. (36) can be alternatively expressed as

$$\hbar\Delta\omega(\mathbf{K}_0) = V_{\mathbf{K}_0\mathbf{K}_0} + \sum_{\mathbf{K}'_\perp \neq \mathbf{K}_{0\perp}} |V_{\mathbf{K}_0\mathbf{K}'}|^2 \times \times \sum_{m=-\infty}^{\infty} N_y J_m^2(\xi)\, G_0[\xi, m, m; \bar{\varepsilon}_{n_0}(\mathbf{K}_{0\perp}) - \bar{\varepsilon}_{n_0}(\mathbf{K}'_\perp)]. \quad (40)$$

Also note that the neglected off-diagonal term on the right-hand side of Eq. (40) [which arises from the neglected term on the right-hand side of Eq. (33)] is expressed in terms of G_0 as

$$\sum_{\mathbf{K}'_\perp \neq \mathbf{K}_{0\perp}} |V_{\mathbf{K}_0\mathbf{K}'}|^2 \sum_{m,m'=-\infty}^{\infty} J_m(\xi) J_{m'}(\xi) \times \times G_0[\xi, m, m'; \bar{\varepsilon}_{n_0}(\mathbf{K}_{0\perp}) - \bar{\varepsilon}_{n_0}(\mathbf{K}'_\perp)]. \quad (41)$$

For convenience of performing the sum over $\mathbf{K}_\perp$, we use the form $\Delta\omega$ expressed in Eq. (36) throughout.

4. Degradation of cavity-enhanced SE: Constant relaxation-time approximation

In this section, for purposes of showing heuristic trends with regard to the effects of interface roughness, the analysis for Eq. (38) is carried out for the *assumed* case where the damping term, Γ, is a constant, independent of $\mathbf{K}$, and the frequency shift is zero. In this case, it follows from Eq. (38) that

$$A_n(\mathbf{K}_0, t) = \int_0^t dt' \dot{A}_q^0(\mathbf{K}_0, t') e^{-(t-t')/\tau}, \quad (42)$$

where $\tau = 2/\Gamma$ takes on the meaning of a characteristic mean dephasing time, and from Eq. (5) it follows that

$$\dot{A}_q^0(\mathbf{K}_0, t) = D(q_x/q)^{1/2} v_y[\mathbf{k}_0(t) - \mathbf{q}_s] \times \times \exp\left\{-\frac{i}{\hbar}\int_0^t \{\varepsilon_{n_0}[\mathbf{k}_0(t_1)] - \varepsilon_{n_0}[\mathbf{k}_0(t_1) - q_s] - \hbar\omega_q\}\, dt_1\right\}. \quad (43)$$

Therefore, the one photon SE probability amplitude can be expressed as

$$A_q(\mathbf{K}_0, t) = A_q^0(\mathbf{K}_0, t, \tilde{\omega}_q) e^{-t/\tau}, \quad (44)$$

where $A_q^0(\mathbf{K}_0, t, \tilde{\omega}_q)$ is obtained from Eq. (5) by the formal substitution of a renormalized *complex* photon "energy" $\hbar\tilde{\omega}_q = \hbar\omega_q - i\hbar\omega_\tau$ in place of $\hbar\omega_q$ with $\omega_\tau \equiv 1/\tau$, so that

$$A_q^0(\mathbf{K}_0, t, \tilde{\omega}_q) = D(q_x/q)^{1/2} \int_0^t dt' v_y[\mathbf{k}_0(t') - \mathbf{q}_s] \times \times \exp\left\{-\frac{i}{\hbar}\int_0^{t'} \{\varepsilon_{n_0}[\mathbf{k}_0(t_1)] - \varepsilon_{n_0}[\mathbf{k}_0(t_1) - \mathbf{q}_s] - \hbar\tilde{\omega}_q\}\, dt_1\right\}. \quad (45)$$

This incorporation of the relaxation-time approximation parameter, ω_τ, as a *complex* addition into the renormalized photon frequency, $\tilde{\omega}_q$, thus allows us to analyze degradation in a straight forward manner. Then the emission process results in the total SE probability

$$P_e^s(t) = \sum_q \sum_{s=1,2} |A_q(\mathbf{K}_0, t)|^2. \quad (46)$$

A. Selection rules

In evaluating $A_q(\mathbf{K}_0, t)$, the external dc field, $\mathbf{E}$, is assumed to be oriented along the y axis; it then follows that $k_{0y}(t) = K_{0y} + eEt/\hbar$. In taking advantage of the periodic properties of the terms in Eq. (45), $A_q(\mathbf{K}_0, t)$ in Eq. (44) is evaluated in *clocked* integral multiples N of the Bloch period, so that $t = N\tau_B$, where $\tau_B = 1/\nu_B = 2\pi/\omega_B$, the time to traverse one period of the Brillouin zone. The integral in Eq. (45) over time can be replaced by an integral over k_{0y} through the substitution $dt = (\hbar/eE)dk_{0y}$. Then the probability amplitude of Eq. (44), evaluated at integral multiples of the Bloch period, can be expressed in terms of the probability amplitude over a single Bloch period, τ_B, [16] to obtain

$$A_q(\mathbf{K}_0, N\tau_B) = \frac{1 - \exp(-iN\tilde{\beta}_q)}{1 - \exp(-i\tilde{\beta}_q)} e^{-(N-1)\tau_B/\tau} A_q(\mathbf{K}_0, \tau_B), \quad (47)$$

where the complex parameter $\tilde{\beta}_q$ is given by

$$\tilde{\beta}_q = 2\pi\frac{\tilde{\omega}_q}{\omega_B} + \frac{1}{eE}\int_{K_{0y}}^{K_{0y}+G_y} dk_{0y}\left[\varepsilon_{n_0}(\mathbf{k}_0) - \varepsilon_{n_0}(\mathbf{k}_0 - \mathbf{q}_s)\right], \quad (48)$$

and $G_y = 2\pi/a$, the y component of the SL reciprocal-lattice vector. From Eq. (47), the corresponding squared probability amplitudes are expressed as

$$|A_q(\mathbf{K}_0, N\tau_B)|^2 = \eta(\omega_q, N, \tau)\, |A_q(\mathbf{K}_0, \tau_B)|^2, \quad (49)$$

where the *transfer* function $\eta(\omega_q, N, \tau)$ is given by

$$\eta(\omega_q, N, \tau) = = \frac{\sinh^2(\pi N/\tau\omega_B) + \sin^2(\pi N\omega_q/\omega_B)}{\sinh^2(\pi/\tau\omega_B) + \sin^2(\pi\omega_q/\omega_B)} e^{-2\pi(N-1)/\tau\omega_B}. \quad (50)$$

Here, η clearly shows the effect of Bloch oscillation dephasing in the constant relaxation-time approximation.

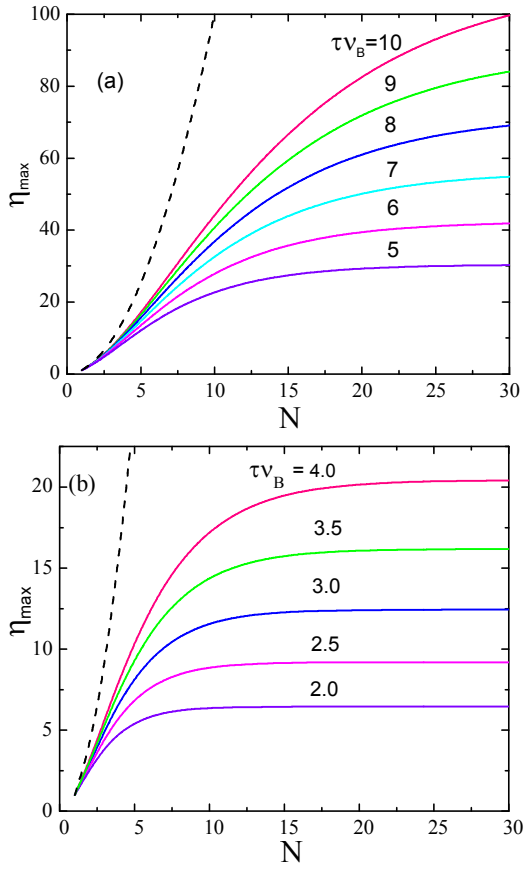

Fig. 1. The transfer function $\eta = \eta(\omega_q, N, \tau)$ calculated at maximum growth conditions [Eq. (51)], $\eta = \eta_{max}$, as a function of a number of Bloch oscillations N for different values of $\tau\nu_B$: (a) $5 \le \tau\nu_B \le 10$ and (b) $2 \le \tau\nu_B \le 4$. The dashed curve shows $\eta_{max} \sim N^2$ without dephasing ($\tau\nu_B \to \infty$).

The general behavior of $\eta(\omega_q, N, \tau)$ is displayed in Fig. 1. From Eqs. (49) and (50), it is seen that for the case of a weak scattering when $\pi N/\tau\omega_B << 1$, i.e., when the electron scattering event is not probable even over many Bloch oscillations, N, on the time scale of the scattering time τ, then the quantity $|A_q(\mathbf{K}_0, N\tau_B)|^2$ will reach its maximum growth value when $\beta_q = 2\pi(m+\delta)$, where $\beta_q = \mathrm{Re}(\tilde{\beta}_q)$, m is an integer and $\delta \to 0$; for this limiting case, the function $\eta(\omega_q, N, \tau)$ is reduced to the function $\eta(\omega_q, N)$ previously obtained in the absence of scattering [16], that is $\eta(\omega_q, N) = \sin^2(N\beta_q/2)/\sin^2(\beta_q/2) \to N^2$, i.e., it becomes sharply peaked at the resonances with increasing N. It is clear that this condition for maximum growth establishes the *selection rules* for both the photon emission frequency, ω_q, and the key wave vector component, q_z,

$$\omega_q = m\omega_B, \quad q_z = q_{zm} \equiv q_x\left[(m\omega_B/\omega_c)^2 - 1\right]^{1/2}; \qquad (51)$$

this gives the *"Stark ladder"* resonance frequency condition, along with the sustaining wave vector cavity resonance conditions. Thus, the modes that radiate with the highest probability correspond to the fundamental Bloch frequency and its harmonics. These quantization conditions are obtained without requiring any assumptions concerning the existence of Wannier-Stark energy states. Further, analyzing the changing behavior of $\eta(\omega_q, N, \tau)$ with increased intensity of scattering, it is noted that the peak positions are negligibly affected, although the associated spectral widths become broadened and related peak values are reduced with decreasing ratio of τ/τ_B (Figs. 1a and 1b). From this *relaxation-time approximation* result, it is noted that the maximum growth condition for the probability amplitudes in Eqs. (49) and (50) still *preserves* the selection rules for SE given in Eq. (51) despite the increased reasonably strong scattering ($\tau\nu_B \ge 1$). It is important to emphasize that both Eqs. (49) and (51) taken together are central to the evaluation of total SE probability.

In the preceding calculation, if $\Delta\omega(\mathbf{K}_0)$ were chosen to be a non-zero constant, say ω_0, then the selection rules in Eqs. (51) would indicate a constant shift in ω_q by the assumed constant ω_0, which would then be appropriately reflected in Eq. (50) by replacing ω_q with $\omega_q + \omega_0$.

Not withstanding the relaxation-time approximation, both $\Delta\omega$ and Γ in Eqs. (36)-(38) are non-trivial functions of **K**-vector and $\hbar\omega_B$, so that depending on the strength and breath of the interface inhomogeneity, the Stark selection rules and the SE will be affected by this dependence. The analysis is extended beyond the relaxation-time approximation in Section V to demonstrate the dependence of Γ and $\Delta\omega$ on **K**-vector and $\hbar\omega_B$ within a model problem.

B. General expression for the total SE probability

The total SE probability at time $t = N\tau_B$, noted as $P_e^s = P_e^s(N\tau_B)$, is evaluated by substituting $|A_q(\mathbf{K}_0, N\tau_B)|^2$ from Eq. (49) into Eq. (46). The sum over q in Eq. (46) is replaced by an integral over q, by taking into account the TE_{10} mode density of states and polarization such that $\sum_q(\cdots) \to (L_z/\pi)\int dq(\cdots)/[1-(q_x/q)^2]^{1/2}$. Thus, P_e^s can be written as

$$P_e^s = \frac{L_z}{\pi}\sum_{s=1,2}\int dq\,\eta(\omega_q, N, \tau)\frac{|A_q(\mathbf{K}_0, \tau_B)|^2}{\left[1-(q_x/q)^2\right]^{1/2}}. \qquad (52)$$

In Eq. (52), we have made use of the mode density of states for a lossless waveguide cavity; this results in infinitely sharp peaks at the system resonances. However, if we incorporate a radiative loss component

into the density of states due to the interaction of the radiation field with lossy cavity waveguide walls, this would lead to a broadening and finiteness of the density of states resonance peaks. Therefore, we introduce here a well-known and frequently used phenomenological Lorentzian broadening component into the density of states, which approximates [38] the effect of radiative dissipation to the cavity walls. As such, the singularity of the density of states in Eq. (52) can be expressed as $1/[1-(q_x/q)^2]^{1/2} = (q/q_x)/(q/q_x+1)^{1/2}(q/q_x-1)^{1/2}$; then, in replacing $(q/q_x-1)^{-1/2}$ by $\lim_{\Gamma_q\to 0}\left[\frac{1}{\Gamma_q^2+(q/q_x-1)^2}\right]^{1/4}$ with $\Gamma_q = 1/2Q$, where Q is the microcavity quality factor, we can express Eq. (52) as

$$P_e^s = \frac{L_z}{\pi}\sum_{s=1,2}\int dq\,\eta(\omega_q,N,\tau)\times \times\frac{q|A_q(\mathbf{K}_0,\tau_B)|^2}{q_x(q/q_x+1)^{1/2}}\left[\frac{1}{\Gamma_q^2+(q/q_x-1)^2}\right]^{1/4}. \quad (53)$$

Thus, P_e^s in Eq. (53) is reflective of the loss component at the resonances.

The integral in Eq. (53) can be evaluated by using the special property of the integrand, that is, $\eta(\omega_q,N,\tau)$ is a sharply peaked, symmetric function of q, at $q = q_m \equiv (q_x^2+q_{zm}^2)^{1/2}$. With decreasing τ, the maximum values of this function decrease relative to the *no scattering case* ($\tau=\infty$). However, its sharp and oscillatory behavior is preserved for the wide range of physical scattering times greater than or of the order of the inverse Bloch frequency ν_B. Thus, for $\tau\nu_B \geq 1$, at every node defined by the resonance conditions, the slowly varying function of q in the integrand, including the peaked density of states, can be replaced by its value evaluated at $q = q_m$, and then removed from the integral over q. It is noted that in comparing the effective half-widths of η and the Lorentzian lineshape, we find that the sharpness of η dominates for the conditions that $\Gamma_q >> \Gamma_N \equiv 1/2Q_N$, $Q << Q_N \equiv \sqrt{15\pi}N$. Within these criteria, the integral over q can be completed as outlined to obtain

$$P_e^s = I_N(\tau\nu_B)\frac{L_z\omega_B}{L_x\omega_c}\sum_{l=1}^{l_{\max}}\sum_{s=1,2}|A_{q_l}^0(\mathbf{K}_0,\tau_B,\tilde{\omega}_{q_l})|^2\times \times\frac{q_l/q_x}{(q_l/q_x+1)^{1/2}}\left[\frac{1}{\Gamma_q^2+(q_l/q_x-1)^2}\right]^{1/4}. \quad (54)$$

Here, $l_{\max}$ follows from $q_{\max} = l_{\max}(\omega_B/\omega_c)q_x$, and determines the upper limit in the sum over higher Bloch oscillation harmonics. The integral $I_N(\tau\nu_B)$ reflects Eq. (50) and is defined by

$$I_N(\tau\nu_B) = e^{-(N+1)/\tau\nu_B}\frac{2}{\pi}\int_0^{\pi/2}dx\frac{\sinh^2(N/2\tau\nu_B)+\sin^2(Nx)}{\sinh^2(1/2\tau\nu_B)+\sin^2(x)}. \quad (55)$$

The calculation of P_e^s in Eq. (54) requires the use of $A_q^0(\mathbf{K}_0,\tau_B,\tilde{\omega}_q)$ in Eq. (45), evaluated at the maximum growth conditions of Eq. (51), that is, when $\hbar\omega_q = m\hbar\omega_B$ and $q = q_m$. In addition, the dependence on q in Eq. (45) is made explicit by invoking the assumption of photon long-wave limit, which is valid for all periodic potentials of interest, even superlattices, where $q = \pi/a$. Thus, Eq. (45) results in

$$A_{q_l}^0(\mathbf{K}_0,\tau_B,\tilde{\omega}_{q_l}) = \frac{2\pi}{\omega_B}\left(\frac{q_x}{q_l}\right)^{1/2}DI_l\exp(-iK_{0y}a\tilde{\omega}_{q_l}/\omega_B), \quad (56)$$

where

$$I_l = \frac{1}{2\pi}\int_{-\pi}^{\pi}d\vartheta_k[v_y(\vartheta_k)\exp(\vartheta_k/2\pi\tau\nu_B)]\exp(il\vartheta_k) \quad (57)$$

is the l-th Fourier component of the function $v_y(\vartheta_k)\exp(\vartheta_k/2\pi\tau\nu_B)$, $\vartheta_k = k_{0y}a$, and $\tilde{\omega}_{q_l} = l\omega_B - i/\tau$. Note that D in Eq. (56) has been defined below Eq. (5). Since the electron velocity component $v_y(\vartheta_k)$ depends on details of the SL miniband structure, such dependence comes explicitly into the SE probability amplitude through the integral I_l given by Eq. (57), thus

$$|A_{q_l}^0(\mathbf{K}_0,\tau_B,\tilde{\omega}_{q_l})|^2 = \frac{q_x}{q_l\nu_B^2}|DI_l|^2\exp(K_{0y}a/\pi\tau\nu_B). \quad (58)$$

Note that the exponential term in Eq. (58) contains a dependence on the initial wave vector, K_{0y}. This dependence is implicit in Eq. (44) through τ and $\tilde{\omega}_q$, and arises from the *symmetry breaking* incorporation of damping into SE probability amplitude analysis. Since $K_{0y}a/\pi$ is bounded within $[-1,1]$ in the Brillouin zone, and $2 \leq \tau\nu_B < \infty$ is the physical range of values taken under circumstances of strong to weak scattering, respectively, a simple estimate shows that for $\tau\nu_B = 2$, the exponential factor varies from approximately 0.61 at $K_{0y} = -\pi/a$ to 1.65 at $K_{0y} = \pi/a$, and for weak scattering, when $\tau\nu_B$ is very large, the exponential factor is approximately unity throughout the Brillouin zone. Therefore, in further discourse, the analysis is treated for the weak scattering case, and the exponential factor is replaced by unity so that Eq. (58) becomes

$$|A^0_{q_l}(\mathbf{K}_0,\tau_B,\widetilde{\omega}_{q_l})|^2 \equiv |A_{q_l}(\tau_B,\widetilde{\omega}_{q_l})|^2 = \frac{q_x}{q_l \nu_B^2}|DI_l|^2. \quad (59)$$

If one wanted to include this exponential factor for strong scattering analysis, then knowledge of the initial condition would be required; in lacking such knowledge, a suitable ensemble average would have to be taken over probable initial conditions to get a weighted average.

C. Analysis of the total SE probability for specific energy miniband

The analysis for SE and radiation characteristics is now developed by considering a general form for the electron energy miniband dispersion relation given by Eq. (20). In particular, the well-known case of NNTB approximation corresponds with purely harmonic energy dispersion where only the single term ($l'=1$) is considered as significant, so that the next nearest neighbor and longer range QW wave function overlaps are assumed to be negligibly small. The electron group velocity in the general miniband of Eq. (20), for the given K_y in the y direction, is then given by $v_y(K_y)=\sum_{l'=1}^{\infty} v_{l'}\sin(l'aK_y)$, where $v_{l'}=l'a\Delta_{l'}/2\hbar$, the maximum velocity associated with the l'-th miniband of band width, $\Delta_{l'}$. Substituting the expression for $v_y(K_y)$ in Eq. (57), one can find the total SE probability from Eqs. (54) and (59) as

$$P_e^s = \frac{2\alpha\varepsilon^{1/2}L_x v_1^2\omega_c}{\pi^2 L_y c^2 \omega_B} I_N(\tau\nu_B)\sinh^2(1/2\tau\nu_B)\times$$
$$\times \sum_{l=1}^{l_{\max}} \frac{|S_l|^2}{(q_l/q_x+1)^{1/2}}\left[\frac{1}{\Gamma_q^2+(q_l/q_x-1)^2}\right]^{1/4}, \quad (60)$$

where $v_1 = a\Delta_1/2\hbar$ and

$$S_l = \sum_{l'=1}^{\infty}\frac{v_{l'}}{v_1}\left\{\frac{\cos[\pi(l'+l)]}{i(l'+l)+1/2\pi\tau\nu_B}+\frac{\cos[\pi(l'-l)]}{i(l'-l)-1/2\pi\tau\nu_B}\right\}. \quad (61)$$

Here, summation is carried out over both the higher harmonics of Bloch frequency (l) and higher harmonics of the general energy miniband (l') from Eqs. (20) and (61).

Let us consider the case of a purely harmonic miniband ($l'=1$) described within the NNTB approximation; in this case, the probability amplitude in Eqs. (59) and (57) results in

$$|A_{q_l}(\tau_B,\widetilde{\omega}_{q_l})|^2 =$$
$$= 4\pi^4 |D|^2 \frac{\omega_c v_1^2}{\omega_B^3 l}\frac{\sinh^2(1/2\tau\nu_B)}{(\pi l/\tau\nu_B)^2+[(1/2\tau\nu_B)^2-\pi^2(l^2-1)]^2}, \quad (62)$$

where an account has been taken for the wave vector $q_l = q_x l\omega_B/\omega_c$. In particular, if finite scattering is totally ignored ($\tau\nu_B\to\infty$), then from Eq. (57) $I_l = i(v_1/2)\delta_{1l}$, and therefore

$$|A_{q_l}(\tau_B,\widetilde{\omega}_{q_l})|^2 \equiv |A_{q_l}(\tau_B)|^2 = \pi^2|D|^2(\omega_c v_1^2/\omega_B^3)\delta_{1l}.$$

Thus, it is concluded that for the electron dynamics in a purely *harmonic* miniband when only the single Fourier component of the electron velocity $v_y(\vartheta_k)$ with $l'=1$ is nonzero, and in the absence of scattering, all probability amplitudes $|A_{q_l}(\tau_B)|^2$ are zero, except the one corresponding to $l=1$. In accordance with the selection rule of Eq. (51), this frequency harmonic corresponds to the fundamental Bloch frequency alone. It is interesting to note that with finite values of scattering time, the generation of higher Bloch harmonics becomes possible even in a pure harmonic miniband. From Eqs. (54) and (62), the total SE probability becomes

$$P_e^s = 8\pi^2\alpha I_N(\tau\nu_B)\varepsilon^{1/2}\frac{L_x}{L_y}\frac{v_1^2}{c^2}\frac{\omega_c}{\omega_B}\times$$
$$\times \sum_{l=1}^{l_{\max}}\frac{\sinh^2(1/2\tau\nu_B)}{(q_l/q_x+1)^{1/2}\left\{(\pi l/\tau\nu_B)^2+[(1/2\tau\nu_B)^2-\pi^2(l^2-1)]^2\right\}}\times$$
$$\times\left[\frac{1}{\Gamma_q^2+(q_l/q_x-1)^2}\right]^{1/4}. \quad (63)$$

It is seen from Eq. (63) that with increasing τ, the effect of higher Bloch harmonics generation becomes reduced, and for $\tau\to\infty$ it completely disappears. In tracking the contribution from higher harmonics of Bloch frequency in the total SE probability, note once again that the NNTB approximation in Eq. (20) is obtained by letting $\Delta_{l'}=\Delta_1\delta_{1l'}$ so that $v_{l'}=v_1\delta_{1l'}$. Occurrence of the Kronecker symbol, $\delta_{1l'}$, allows for the contribution of the $l'=1$ term only, whereas all other terms are equal to zero, thereby limiting, within the NNTB approximation and without scattering, generation to the fundamental Bloch harmonic. In this problem, the genesis of harmonics arises from the basic structure of the probability amplitude in Eqs. (42), (43); these equations have a direct dynamical dependence on the Bloch electron velocity and the SL miniband energy, both of which contain a broad harmonic dependence due to band periodicity. However, as noted from Eqs. (60) and (61), in the relaxation-time approximation, finite scattering plays a role, but as $\tau\to\infty$, only the pure harmonic survives.

D. Total SE power estimate

Spontaneous emission is considered for photon energy $\hbar\omega_q = \hbar\omega_B$ corresponding to the fundamental Bloch

harmonic frequency. It follows from Eq. (63) that the SE probability for $l=1$ is given by

$$P_e^s(l=1,\tau)=8\pi^2\alpha I_N(\tau\nu_B)\varepsilon^{1/2}\frac{L_x}{L_y}\frac{v_1^2}{c^2}\frac{\omega_c}{\omega_B}\times$$
$$\times\frac{\sinh^2(1/2\tau\nu_B)}{(q/q_x+1)^{1/2}[(\pi/\tau\nu_B)^2+(1/2\tau\nu_B)^4]}\times \qquad (64)$$
$$\times\left[\frac{1}{\Gamma_q^2+(q/q_x-1)^2}\right]^{1/4}.$$

In the absence of scattering, Eq. (64) is evaluated in the limit $\tau\nu_B\to\infty$ to get

$$P_e^s(l=1,\tau\nu_B\to\infty)=2\alpha N\varepsilon^{1/2}\frac{L_x}{L_y}\frac{v_1^2}{c^2}\frac{\omega_c}{\omega_B(\omega_B/\omega_c+1)^{1/2}}\times$$
$$\times\left[\frac{1}{\Gamma_q^2+(\omega_B/\omega_c-1)^2}\right]^{1/4}; \qquad (65)$$

indeed, for the limit of $\tau\nu_B\to\infty$, the integral in Eq. (55) behaves as a linear function of N, that is,

$$I_N(\tau\nu_B\to\infty)\to(2/\pi)\int_0^{\pi/2}\frac{\sin^2(Nx)}{\sin^2(x)}dx=N,$$

so that Eq. (64) goes over to Eq. (65). For finite values of τ, the linear dependence of $P_e^s(N)$ is replaced by the general factor $I_N(\tau\nu_B)$, which is a *slower than linear*, but an increasing function of N. To compare the probabilities for SE with and without scattering, we obtain the ratio

$$P_r\equiv\frac{P_e^s(l=1,\tau)}{P_e^s(l=1,\tau\nu_B\to\infty)}=$$
$$=\frac{1}{N}I_N(\tau\nu_B)\frac{\sinh^2(1/2\tau\nu_B)}{(1/2\tau\nu_B)^2[1+(1/4\pi\tau\nu_B)^2]}. \qquad (66)$$

In particular, for frequencies close to the peak of the density of states ($\omega_B\cong\omega_c$), we get from Eq. (65) in the absence of scattering

$$P_e^s(l=1,\tau\nu_B\to\infty,\omega_B=\omega_c)=\frac{3}{\pi}(\varepsilon Q)^{1/2}P_{fs}, \qquad (67)$$

where $P_{fs}=(2\pi/3)\alpha N v_1^2/c^2$ is the probability of SE into free space. Hence, the enhancement of SE probability into the microcavity waveguide relative to SE into free space, $P_c(\tau\nu_B\to\infty)\equiv P_e^s(l=1,\tau\nu_B\to\infty,\omega_B=\omega_c)/P_{fs}$ is determined by

$$P_c(\tau\nu_B\to\infty)=\frac{3}{\pi}(\varepsilon Q)^{1/2}, \qquad (68)$$

i.e., the Purcell factor proportional to $Q^{1/2}$. Similarly, for a finite τ, it follows from Eq. (64) that

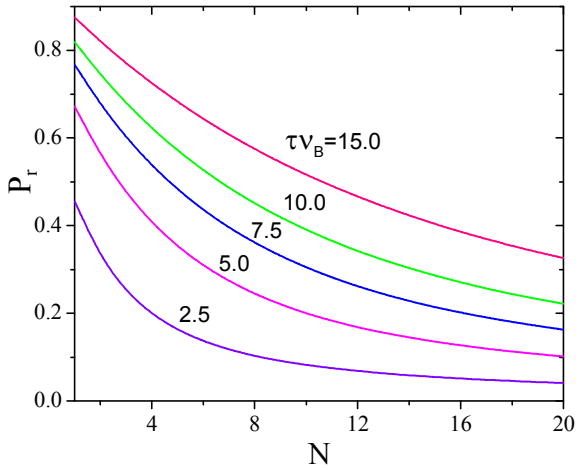

Fig. 2. Relative SE probability P_r [Eq. (66)] as a function of N at fundamental Bloch frequency for different values of $\tau\nu_B$.

$$P_e^s(l=1,\tau,\omega_B=\omega_c)=$$
$$=P_{fs}P_c(\tau\nu_B\to\infty)P_r=P_c(\tau)P_{fs}, \qquad (69)$$

where the relative probability $P_c(\tau)\equiv P_e^s(l=1,\tau,\omega_B=\omega_c)/P_{fs}$ is given by $P_c(\tau)=P_c(\tau\nu_B\to\infty)P_r$. The latter clearly reflects both the effects of the microcavity waveguide $[P_c(\tau\nu_B\to\infty)]$ and the electron scattering (P_r). Depending on the operational parameters Q and $\tau\nu_B$, either factor in Eq. (69) can dominate in which case inhibition $[P_c(\tau)<1]$ or enhancement $[P_c(\tau)>1]$ can take place. Then, assuming the enhancement of the total probability in Eq. (69) $P_c(\tau)>1$, we get the criterion on the quality factor $Q>Q_0(\tau\nu_B)$, where $Q_0(\tau\nu_B)=(\pi/3)^2/\varepsilon P_r^2$ is determined from the equation $P_c(\tau)=1$. Combining both criteria [see discussion above Eq. (54)], we get the region for Q values which is determined as follows $Q_0(\tau\nu_B)<Q<<Q_N$.

The relative SE probability, P_r, calculated as a function of N at different values of the dephasing parameter $\tau\nu_B$, is shown in Fig. 2; within the relaxation-time approximation, it is seen that the effect of dephasing on the relative total SE probability becomes more prominent with decreased $\tau\nu_B$. As a numerical estimate, assume that $\tau\nu_B=10$ and $N=10$, which corresponds to the aspect ratio of $\tau\nu_B/N=1$. Then in using the data of Fig. 2 with the curve indicated by $\tau\nu_B=10$, one obtains $P_r\cong0.39$ for $N=10$; then it follows that the total SE probability and the generated output power of SE is appreciably damped by a factor of 2.6 due to dephasing effects as compared with that in the absence of scattering. To obtain a specific value for

power output, use is made of the conditions for a GaAs-based SL ($\varepsilon = 12.2$) with the miniband width $\Delta = 36\,\text{meV}$, the SL period $a = 10\,\text{nm}$, the vertical dimension $14\,\mu\text{m}$, and the lateral cross section $28\times1000\ \mu\text{m}^2$ embedded into a rectangular waveguide. For the estimate, the electron density is taken to be $5\cdot10^{16}\,\text{cm}^{-3}$, which provides the total number of electrons $n = 2\times10^{10}$ in the active region of SL. The Bloch frequency $\nu_B (\cong \nu_c) = 1.5\,\text{THz}$ corresponds to $\hbar\omega_B \cong 6\,\text{meV}$ and the electric field $E = \hbar\omega_B/ea = 6$ kV/cm, which requires the external bias of 8.4 V. The SE power generated into free space is estimated to be $W_{fs} = (\hbar\omega_B n/N\tau_B) P_{fs} \cong 0.36\,\mu\text{W}$. The Purcell factor is estimated as $P_c(\tau\nu_B \to \infty) \cong 10$ for $Q = 9$ ($Q_0 \cong 0.6$, $Q_N \cong 69$); then we get $P_c(\tau) \cong 3.9$. This results in the estimate of the damped SE power generated into the microcavity environment under the dephasing effects $W_\tau \cong 1.4\,\mu\text{W}$. The estimates show that the SE power of about $1\,\mu\text{W}$ is achievable for the microcavity quality factor in the range of 4-5; this shows the degradation effects from SLIR can be more than compensated for by the enhancements derived from mircocavity-based confinement tuning.

5. Localized interface roughness model

In proceeding beyond the relaxation-time approximation, consideration is now given to the more general result of Eqs. (36) and (37) where the interface roughness model is explored, that is, the lattice comb of localized planar interface inhomogeneities with randomly distributed planar interface roughness defined by an ensemble averaged autocorrelation function (9) and (10). Clearly the results of evaluating Eqs. (36) and (37) explicitly will differ from the constant relaxation-time approximation in that both $\Delta\omega(\mathbf{K}_0)$ and $\Gamma(\mathbf{K}_0)$ are non-trivial functions of wave vector $\mathbf{K}_0$. As such, it has been explicitly shown in Sec. III that the matrix elements for this lattice comb are given in Eqs. (8) and (27) from which one can arrive at

$$\langle|V_{\mathbf{KK}'}|^2\rangle = \frac{1}{N_0^2}\sum_{\mathbf{l},\mathbf{l}'}\langle v(\mathbf{l})v^*(\mathbf{l}')\rangle e^{i(\mathbf{K}-\mathbf{K}')\cdot(\mathbf{l}-\mathbf{l}')}. \tag{70}$$

This ensemble average matrix element can be re-expressed by opening the sums over $\mathbf{l}$ and $\mathbf{l}'$ in terms of y and perpendicular components so that Eq. (70) becomes

$$\langle|V_{\mathbf{KK}'}|^2\rangle = \frac{1}{N_y^2}\sum_{l_y,l_y'}\frac{1}{N_\perp^2}\times \times\sum_{\mathbf{l}_\perp,\mathbf{l}_\perp'}\langle v(l_y,\mathbf{l}_\perp)v^*(l_y',\mathbf{l}_\perp')\rangle e^{i(\mathbf{K}-\mathbf{K}')\cdot[(l_y-l_y')\hat{\mathbf{j}}+(\mathbf{l}_\perp-\mathbf{l}_\perp')]}. \tag{71}$$

In general, the matrix elements in Eq. (71) can be separated into planar, $\langle|V_{\mathbf{KK}'}|^2\rangle_p$, and cross-planar, $\langle|V_{\mathbf{KK}'}|^2\rangle_{cp}$, contributions as $\langle|V_{\mathbf{KK}'}|^2\rangle = \langle|V_{\mathbf{KK}'}|^2\rangle_p + \langle|V_{\mathbf{KK}'}|^2\rangle_{cp}$, where

$$\langle|V_{\mathbf{KK}'}|^2\rangle_p = \frac{1}{N_y^2}\sum_{l_y}\frac{1}{N_\perp^2}\times \times\sum_{\mathbf{l}_\perp,\mathbf{l}_\perp'}\langle v(l_y,\mathbf{l}_\perp)v^*(l_y,\mathbf{l}_\perp')\rangle e^{i(\mathbf{K}-\mathbf{K}')\cdot(\mathbf{l}_\perp-\mathbf{l}_\perp')} \tag{72}$$

comes from independent planar interfaces and

$$\langle|V_{\mathbf{KK}'}|^2\rangle_{cp} = \frac{1}{N_y^2}\sum_{l_y\neq l_y',l_y'}\frac{1}{N_\perp^2}\times \times\sum_{\mathbf{l}_\perp,\mathbf{l}_\perp'}\langle v(l_y,\mathbf{l}_\perp)v^*(l_y',\mathbf{l}_\perp')\rangle e^{i(\mathbf{K}-\mathbf{K}')\cdot[(l_y-l_y')\hat{\mathbf{j}}+(\mathbf{l}_\perp-\mathbf{l}_\perp')]} \tag{73}$$

takes into account cross-correlations between different planar interfaces. The planar and cross-planar contributions to the matrix elements are established below in Secs. A and B, respectively, along with their contributions to the damping constant, Γ, and the frequency shift, $\Delta\omega$.

A. Roughness effects from independent planar interfaces

For independent planar interfaces, then making use of the autocorrelation relation (9) in Eq. (72), one obtains

$$\langle|V_{\mathbf{KK}'}|^2\rangle_p = \frac{1}{N_y^2}\sum_{l_y}\langle|v(l_y)|^2\rangle\frac{1}{N_\perp^2}\times \times\sum_{\mathbf{l}_\perp,\mathbf{l}_\perp'}e^{-(\mathbf{l}_\perp-\mathbf{l}_\perp')^2/\Lambda_y^2}e^{i(\mathbf{K}_\perp-\mathbf{K}_\perp')\cdot(\mathbf{l}_\perp-\mathbf{l}_\perp')}. \tag{74}$$

The double sum $\frac{1}{N_\perp^2}\sum_{\mathbf{l}_\perp,\mathbf{l}_\perp'}$ in Eq. (74) can be evaluated by using the Poisson summation formula. Specifically, the double sums over areal vectors $\mathbf{l}_\perp = l_x\hat{\mathbf{i}} + l_z\hat{\mathbf{k}}$ and $\mathbf{l}_\perp' = l_x'\hat{\mathbf{i}} + l_z'\hat{\mathbf{k}}$ can be further decomposed into four sums over $l_x = n_x a_x$, $l_x' = n_x' a_x$; $l_z = n_z a_z$, and $l_z' = n_z' a_z$, where n_i are the number of cells and a_i are the directional lattice parameters for each perpendicular direction. Then, in the limit of large n_i in each direction perpendicular to the SL axis, the double sum in Eq. (74) is decomposed into $\sum_{l_x,l_x'}$ and $\sum_{l_z,l_z'}$ and evaluated separately by the method of Poisson summation formula [39] to obtain

$$S_i = N_i\Lambda_y\frac{\sqrt{\pi}}{a_i}\sum_{m=-\infty}^{\infty}e^{-\kappa_i^2\Lambda_y^2\left(1+\frac{G_i}{\kappa_i}m\right)^2\Big/4}, \tag{75}$$

for each of the sums. Here, $G_i = 2\pi/a_i$ is the i-th component of the reciprocal lattice vector and κ_i is the i-th component of $(\mathbf{K}_\perp - \mathbf{K}'_\perp)$. For lattices with $a_i \cong 5.7$Å, $G_i \cong 1.1\times10^{10}\,\mathrm{m}^{-1}$ which is much larger than any scattering component, κ_i, in the perpendicular direction; thus $G_i/|\kappa_i| >> 1$ and the only significant term contributing to the sum of exponential terms in Eq. (75) corresponds to the term when $m = 0$. Thus, $S_i = N_i\Lambda_y \dfrac{\sqrt{\pi}}{a_i}\exp(-\kappa_i^2\Lambda_y^2/4)$ and the double sum in Eq. (74) can be expressed as

$$I \equiv \frac{1}{N_\perp^2}\sum_{\mathbf{l}_\perp,\mathbf{l}'_\perp} e^{-(\mathbf{l}_\perp-\mathbf{l}'_\perp)^2/\Lambda_y^2} e^{i(\mathbf{K}_\perp-\mathbf{K}'_\perp)\cdot(\mathbf{l}_\perp-\mathbf{l}'_\perp)} = \pi\frac{\Lambda_y^2}{S_\perp}e^{-\kappa^2\Lambda_y^2/4}; \tag{76}$$

here, $\kappa = |\mathbf{K}_\perp - \mathbf{K}'_\perp|$, $S_\perp = N_\perp a_x a_z$, and $N_\perp = N_x N_z$. Therefore, Eq. (74) becomes

$$\langle|V_{\mathbf{KK}'}|^2\rangle_p = \frac{\pi}{N_y^2 S_\perp}\sum_{l_y}\langle|v(l_y)|^2\rangle\Lambda_y^2 e^{-\kappa^2\Lambda_y^2/4}, \tag{77}$$

summed over the **y** direction of the SL layers. Therefore, at each SL layer, the ensemble averaged matrix elements depend only on the perpendicular components of $\mathbf{K}$ and $\mathbf{K}'$. In addition, $\overline{\varepsilon_{n_0}(\mathbf{K})} - \overline{\varepsilon_{n_0}(\mathbf{K}')}$ from Eq. (12) becomes $\bar{\varepsilon}_{n_0}(\mathbf{K}_\perp) - \bar{\varepsilon}_{n_0}(\mathbf{K}'_\perp)$, which depends only on the perpendicular component of wave vector in the Brillouin zone. Therefore, $\Delta\omega(\mathbf{K}_0)$ and $\Gamma(\mathbf{K}_0)$ can be rewritten in terms of the perpendicular contributions as $\Delta\omega(\mathbf{K}_{0\perp})$ and $\Gamma(\mathbf{K}_{0\perp})$.

Analysis of the type of matrix elements reflected in Eq. (77) have been reported for a model square-well SL [30]. For the simple model case considered in this work, $|v(l_y)|^2$ is essentially constant at all interface sites, so that the ensemble averaged matrix elements from Eq. (77) can be simplified as $\langle|V_{\mathbf{KK}'}|^2\rangle_p = (\pi\Lambda^2/N_y S_\perp)v^2\exp(-\kappa^2\Lambda^2/4)$, with the measure of interface roughness at each interface site reduced to the statistical parameters $\langle|v(l_y)|^2\rangle = v^2$ and $\Lambda_y = \Lambda$. In this case, Eqs. (36) and (37) become

$$\Delta\omega_p(\mathbf{K}_{0\perp}) = \frac{\pi a\Lambda^2 v^2}{\hbar\Omega}\sum_{m=-\infty}^{\infty} R_m \times \times \sum_{\mathbf{K}'_\perp\neq\mathbf{K}_{0\perp}} \frac{e^{-\Lambda^2(\mathbf{K}_{0\perp}-\mathbf{K}'_\perp)^2/4}}{\bar{\varepsilon}_{n_0}(\mathbf{K}_{0\perp}) - \bar{\varepsilon}_{n_0}(\mathbf{K}'_\perp) - m\hbar\omega_\mathrm{B}} \tag{78}$$

and

$$\Gamma_p(\mathbf{K}_{0\perp}) = \frac{2\pi^2 a\Lambda^2 v^2}{\hbar\Omega}\sum_{m=-\infty}^{\infty} R_m \sum_{\mathbf{K}'_\perp\neq\mathbf{K}_{0\perp}} e^{-\Lambda^2(\mathbf{K}_{0\perp}-\mathbf{K}'_\perp)^2/4} \times \times \delta[\bar{\varepsilon}_{n_0}(\mathbf{K}_{0\perp}) - \bar{\varepsilon}_{n_0}(\mathbf{K}'_\perp) - m\hbar\omega_\mathrm{B}], \tag{79}$$

where $\Omega = aN_y S_\perp$ and $\bar{\varepsilon}_{n_0}(\mathbf{K}_\perp)$ comes from Eq. (21) and depends on the specific perpendicular component of the band structure for the material under study.

As a model calculation of Γ_p in Eq. (79), it is assumed that $\bar{\varepsilon}_{n_0}(\mathbf{K}_\perp)$ is given by Eq. (21), and, for simplicity, it is also assumed that $\varepsilon_\perp(\mathbf{K}_\perp) = \hbar^2 K_\perp^2/2m_\perp$. The delta function in Eq. (79) can be expressed as

$$\delta[\bar{\varepsilon}_{n_0}(\mathbf{K}_{0\perp}) - \bar{\varepsilon}_{n_0}(\mathbf{K}'_\perp) - m\hbar\omega_\mathrm{B}] = = \frac{2m_\perp}{\hbar^2}\delta\left(K'^2_\perp - K^2_{0\perp} + \frac{2m_\perp}{\hbar^2}m\hbar\omega_\mathrm{B}\right)$$

and $\sum_{\mathbf{K}_\perp} = \dfrac{S_\perp}{(2\pi)^2}\int d\mathbf{K}_\perp$. Using the property of the delta function, the sum over $\mathbf{K}'_\perp$ alone, namely,

$$I_\Gamma(\mathbf{K}_{0\perp}) = \sum_{\mathbf{K}'_\perp\neq\mathbf{K}_{0\perp}} e^{-\Lambda^2(\mathbf{K}_{0\perp}-\mathbf{K}'_\perp)^2/4} \times \times \delta[\bar{\varepsilon}_{n_0}(\mathbf{K}_{0\perp}) - \bar{\varepsilon}_{n_0}(\mathbf{K}'_\perp) - m\hbar\omega_\mathrm{B}] \tag{80}$$

can be expressed as

$$I_\Gamma(K_{0\perp}) = \frac{S_\perp m_\perp}{2\pi\hbar^2} I_0(\beta_m) e^{-\Lambda^2\left(K_{0\perp}^2 - \frac{m_\perp}{\hbar^2}m\hbar\omega_\mathrm{B}\right)/2}, \tag{81}$$

where $I_n(\beta_m)$ is the modified Bessel function of the first kind of integral order n, $I_n(x) = J_n(ix)$, and

$$\beta_m = \frac{\Lambda^2}{2}K_{0\perp}\left(K_{0\perp}^2 - \frac{2m_\perp}{\hbar^2}m\hbar\omega_\mathrm{B}\right)^{1/2}.$$

The expression for $I_\Gamma(K_{0\perp})$ of Eq. (81) can now be inserted into Eq. (79) and summed over m under the restriction on m imposed by the delta function condition, namely that

$$\frac{\hbar^2}{2m_\perp}(K'^2_\perp - K^2_{0\perp}) + m\hbar\omega_\mathrm{B} = 0.$$

Since

$$\frac{\hbar^2}{2m_\perp}K'^2_\perp = \frac{\hbar^2}{2m_\perp}K^2_{0\perp} - m\hbar\omega_\mathrm{B} \geq 0,$$

it follows that $m \leq m_u \equiv [\hbar K_{0\perp}^2/2m_\perp\omega_\mathrm{B}]$. Here, m_u imposes an upper limit on the possible values of m in the set $\{-\infty,\infty\}$, and $[x]$ is the greatest integer function of x. In addition, $m = 0$ must be excluded from the sum over m, for then, the term $K'_\perp = K_{0\perp}$ would necessarily

be dropped from the sum over $\mathbf{K}'_\perp$ in Eq. (79) as required. Thus, $\Gamma_p(\mathbf{K}_{0\perp}) = \Gamma_p(K_{0\perp})$ in Eq. (79) can be expressed as

$$\Gamma_p(K_{0\perp}) = \Gamma_0 \sum_{m=-\infty}^{m_u} \sigma_m I_0(\beta_m)\, e^{(m\hbar\omega_B - \hbar^2 K_{0\perp}^2/m_\perp)/\varepsilon_\lambda}, \qquad (82)$$

where $m \neq 0$ is imposed in the sum over m. $\Gamma_0 = 2\pi v^2/\hbar\varepsilon_\lambda$, $\varepsilon_\lambda = \hbar^2(\Lambda/2)^{-2}/2m_\perp$ is the size quantization energy associated with the length $\Lambda/2$, and

$$\sigma_m(\xi) = \frac{1}{N_y} R_m(\xi) = \sum_{m'=-\infty}^{\infty} J_{m'}^2(\xi) J_{m'+m}^2(\xi). \qquad (83)$$

In Eq. (83), note that $\sigma_{-m}(\xi) = \sigma_m(\xi)$ and $R_m(\xi)$ is defined in Eq. (33). A graphic analysis of $\sigma_m(\xi)$ is depicted in Fig. 3; a plot of $\sigma_m(\xi)$ versus ξ in the interval $1 \le \xi \le 5$ for m values 1, 2, 3 shows a peaked and decreasing oscillatory behavior, which is a general trend inherent in this quantity.

For the special case where $K_{0\perp} = 0$, then $m_u = 0$, $\beta_m = 0$, and $I_0(0) = 1$; thus, Eq. (82) reduces to $\Gamma_p(0) = \Gamma_0 \sum_{m=1}^{\infty} \sigma_m(\xi) e^{m\hbar\omega_B/\varepsilon_\lambda}$. For convenience in further numerically analyzing $\Gamma_p(0)$, it is scaled in terms of two variables $\zeta = \Delta/\varepsilon_\lambda$ and $\xi = \Delta/2\hbar\omega_B$, where $\Delta \equiv \Delta_1$ is the miniband width. As such, it is re-expressed as

$$\frac{\Gamma_p(0)}{\Gamma'_0} = \zeta \sum_{m=1}^{\infty} \sigma_m(\xi) e^{-mx/2\xi}, \qquad (84)$$

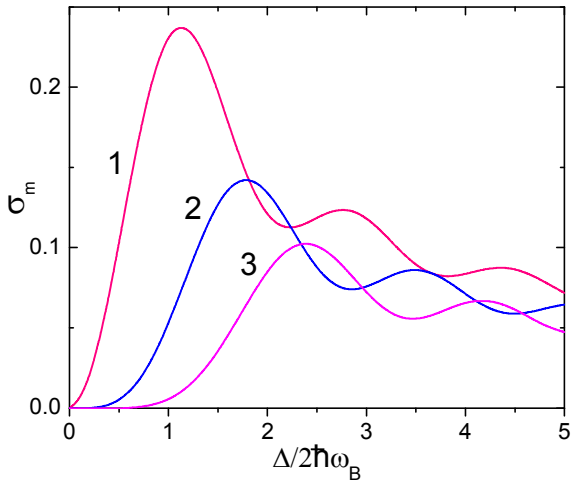

Fig. 3. The dependences of $\sigma_m(\xi)$ [Eq. (83)] as a function of $\xi = \Delta/2\hbar\omega_B$ for the first three values of m in Eq. (84): $m = 1$ (curve *1*), $m = 2$ (*2*), and $m = 3$ (*3*).

where $1/\Gamma'_0 = \tau_0 \equiv \hbar\Delta/2\pi v^2$. The relaxation rate $\Gamma_p(0) = \Gamma_p(\zeta, \xi = \text{const})$ as a function of ζ has a maximum, $\Gamma_{\max}$, at $\zeta = \zeta_{\max}$, which can be found from the equation $\frac{d}{d\zeta}\Gamma_p(\zeta) = 0$. An approximate analytic solution is easily obtained, if we keep only one term in the sum over m ($m = 1$); then $\zeta_{\max} = 2\xi$ and $\Gamma_{\max} = (2/e)\Gamma'_0 \xi\sigma_1(\xi)$. The dependences of $\Gamma_p(\zeta)/\Gamma'_0$, calculated for different values of ξ, and $\Gamma_p(\xi)/\Gamma'_0$, calculated for different values of ζ, are plotted in Figs 4 and 5, respectively. If using numerical parameters from Sec. 4D, that is $\hbar\omega_B = 6$ meV and $\Delta = 36$ meV ($\xi = 3$), we can make an estimate of the relaxation time $\tau = 2/\Gamma$. In particular, we find $\Gamma(\zeta_{\max})/\Gamma'_0 \cong 0.36$ at the maximum point $\zeta_{\max} \cong 4.2$ (Fig. 4, curve 3); thus we obtain the correlation length $\Lambda = \hbar(2\zeta_{\max}/m_\perp\Delta)^{1/2} \cong 16$ nm and the relaxation time $\tau \cong 5.5\tau_0$. Fig. 6 displays the parameter τ_0 versus v. If we take $v = 1.4$ meV, then we get an estimate $\tau_0 \cong 1.8$ ps which gives the relaxation time $\tau \cong 10$ ps.

In evaluating $\Delta\omega_p(\mathbf{K}_{0\perp})$ expressed in Eq. (78), one proceeds in a similar fashion as done in Eqs. (80) and (81); the sum over $\mathbf{K}'_\perp$ in Eq. (78) is evaluated with care taken of the principal value ($\mathbf{K}'_\perp \neq \mathbf{K}_{0\perp}$) and attention is given to lower limit of $\mathbf{K}'_\perp$ determined by $\bar{\varepsilon}_{n_0}(\mathbf{K}_\perp) = \varepsilon_c + \varepsilon_\perp(\mathbf{K}_\perp)$ [see Eq. (21)], where $\varepsilon_c = \varepsilon_{n_0}(0) + \Delta/2$ is the bottom of the band. The sum over $\mathbf{K}'_\perp$ alone in Eq. (78), namely,

$$I_{\Delta\omega}(\mathbf{K}_{0\perp}) = \sum_{\mathbf{K}'_\perp \neq \mathbf{K}_{0\perp}} \frac{e^{-\Lambda^2(\mathbf{K}_{0\perp} - \mathbf{K}'_\perp)^2/4}}{\bar{\varepsilon}_{n_0}(\mathbf{K}_{0\perp}) - \bar{\varepsilon}_{n_0}(\mathbf{K}'_\perp) - m\hbar\omega_B} \qquad (85)$$

can be expressed as

$$I_{\Delta\omega}(K_{0\perp}) = -\frac{S_\perp m_\perp}{2\pi\hbar^2} e^{-[\bar{\varepsilon}_{n_0}(K_{0\perp}) - \varepsilon_c]/\varepsilon_\lambda} I_{\Delta\omega}^{(m)}; \qquad (86)$$

here

$$I_{\Delta\omega}^{(m)} = \int_{x_c}^{\infty} e^{-x} I_0[\mu(x)] \frac{dx}{x + x_m}, \qquad (87)$$

$x = \bar{\varepsilon}_{n_0}(K_\perp)/\varepsilon_\lambda$, $x_c = \varepsilon_c/\varepsilon_\lambda$, $x_m = [m\hbar\omega_B - \bar{\varepsilon}_{n_0}(K_{0\perp})]/\varepsilon_\lambda$, and $\mu(x) = 2(x - x_c)^{1/2}\varepsilon_\perp^{1/2}(K_{0\perp})/\varepsilon_\lambda^{1/2}$. Thus Eq. (78) reduces to

$$\Delta\omega_p(K_{0\perp}) = -\frac{1}{2\pi}\Gamma_0 e^{-[\bar{\varepsilon}_{n_0}(K_{0\perp}) - \varepsilon_c]/\varepsilon_\lambda} \sum_{m=-\infty}^{\infty} \sigma_m I_{\Delta\omega}^{(m)}. \qquad (88)$$

B. Roughness effects from cross-correlated neighboring planar interfaces

The planar contribution to the matrix elements, $\langle|V_{\mathbf{KK}'}|^2\rangle_p$, has already been established in Sec. A, along with its contribution to Γ in Eq. (84) and $\Delta\omega$ in Eq. (88). The evaluation of $\langle|V_{\mathbf{KK}'}|^2\rangle_{cp}$ in Eq. (73), and, therefore, its contribution to Γ, is strongly dependent on the cross-autocorrelation function given by $\langle v(l_y,\mathbf{l}_\perp)v^*(l'_y,\mathbf{l}'_\perp)\rangle$. There is a great discussion of interface roughness models for autocorrelation functions in multilayer systems [20, 40, 41], especially with regard to analysis of X-ray scattering [40]. Here, we make use of an approach motivated by X-ray scattering analysis which considers the cross-correlation function to be approximated as

$$\langle v(l_y,\mathbf{l}_\perp)v^*(l'_y,\mathbf{l}'_\perp)\rangle \cong [\langle v(l_y,\mathbf{l}_\perp)\times v^*(l_y,\mathbf{l}'_\perp)\rangle\langle v(l'_y,\mathbf{l}_\perp)v^*(l'_y,\mathbf{l}'_\perp)\rangle]^{1/2} e^{-d_{yy'}/\delta_{yy'}}, \quad (89)$$

where $\langle v(l_y,\mathbf{l}_\perp)v^*(l_y,\mathbf{l}'_\perp)\rangle$ and $\langle v(l'_y,\mathbf{l}_\perp)v^*(l'_y,\mathbf{l}'_\perp)\rangle$ are given by Eq. (9) for both l_y and l'_y; also $d_{yy'}$ is the thickness of layer $y-y'$, and $\delta_{yy'}$ is the cross-correlation length for layer $y-y'$.

Thus, putting the cross-correlation term of Eq. (89) into $\langle|V_{\mathbf{KK}'}|^2\rangle_{cp}$ of Eq. (73), and summing over $\sum_{\mathbf{l}_\perp,\mathbf{l}'_\perp}$ as in Eq. (76), we obtain

$$\langle|V_{\mathbf{KK}'}|^2\rangle_{cp} = \frac{\pi}{N_y^2 S_\perp}\times \times \sum_{l_y\neq l'_y,l'_y} A_{y,y'}L_{y,y'}^2 e^{-\kappa^2 L_{y,y'}^2/4} e^{i(K_y-K'_y)(l_y-l'_y)}, \quad (90)$$

where $A_{y,y'} = \langle|v(l_y)|\rangle\langle|v(l'_y)|\rangle\exp\left(-d_{yy'}/\delta_{yy'}\right)$, $L_{y,y'}^{-2} = (1/2)(\Lambda_y^{-2}+\Lambda_{y'}^{-2})$, and $l_y = a\ell_y$ with ℓ_y an integer. Then, in placing $\langle|V_{\mathbf{K}_0\mathbf{K}'}|^2\rangle_{cp}$ into Eqs. (36) and (37) and performing the separate sum over K'_y from $\sum_{\mathbf{K}'\neq\mathbf{K}_0} = \sum_{K'_y\neq K_{0y}}\sum_{\mathbf{K}'_\perp\neq\mathbf{K}_{0\perp}}$, we obtain the additions to Γ and $\Delta\omega$ for cross-correlation contributions as

$$\Gamma_{cp}(\mathbf{K}_0) = \frac{2\pi}{\hbar}\sum_{l_y\neq l'_y,l'_y} A_{y,y'}\sum_{m=-\infty}^{\infty}\widetilde{R}_{m,y-y'}\times \times \sum_{\mathbf{K}'_\perp\neq\mathbf{K}_{0\perp}} |\widetilde{V}_{\mathbf{K}_0\mathbf{K}'}|_{cp}^2\,\delta[\bar{\varepsilon}_{n_0}(\mathbf{K}_{0\perp})-\bar{\varepsilon}_{n_0}(\mathbf{K}'_\perp)-m\hbar\omega_B] \quad (91)$$

and

$$\Delta\omega_{cp}(\mathbf{K}_0) = \frac{1}{\hbar}\sum_{l_y\neq l'_y,l'_y} A_{y,y'}\sum_{m=-\infty}^{\infty}\widetilde{R}_{m,y-y'}\times \times \sum_{\mathbf{K}'_\perp\neq\mathbf{K}_{0\perp}} \frac{|\widetilde{V}_{\mathbf{K}_0\mathbf{K}'}|_{cp}^2}{\bar{\varepsilon}_{n_0}(\mathbf{K}_{0\perp})-\bar{\varepsilon}_{n_0}(\mathbf{K}'_\perp)-m\hbar\omega_B}; \quad (92)$$

here

$$\widetilde{R}_{m,s}(\xi) = N_y\sum_{m'=-\infty}^{\infty} J_{m'}(\xi)J_{m'+m}(\xi)J_{m'+s}(\xi)J_{m'+m+s}(\xi) \quad (93)$$

and $|\widetilde{V}_{\mathbf{K}_0\mathbf{K}'}|_{cp}^2 = (\pi/N_y^2S_\perp)L_{y,y'}^2\exp\left(-\kappa^2L_{y,y'}^2/4\right)$. The equation (91) can be reduced to the form of the planar contribution in Eq. (82) by using the same procedure [see Eqs. (80)-(82)] and taking $\langle|v(l_y)|\rangle = v$, $\Lambda_y = \Lambda$, $\delta_{yy'} = \delta$ for all y and y' so that

$$\Gamma_{cp}(K_{0\perp}) = \Gamma_0\sum_{m=-\infty}^{m_u}\widetilde{\sigma}_m I_0(\beta_m)\, e^{(m\hbar\omega_B-\hbar^2K_{0\perp}^2/m_\perp)/\varepsilon_\lambda}, \quad (94)$$

where

$$\widetilde{\sigma}_m(\xi) = 2\sum_{s=1}^{s_u} e^{-as/\delta}\,\widetilde{\sigma}_{m,s}(\xi); \quad (95)$$

here, $\widetilde{\sigma}_{m,s}(\xi) = (1/N_y)\widetilde{R}_{m,s}(\xi)$ and $\widetilde{\sigma}_{-m,s}(\xi) = \widetilde{\sigma}_{m,s}(\xi)$. Also, the upper limit of the index s, $s_u = 2\xi-2$, is determined by the criterion that the number of interfaces crossed within the Bloch oscillation, $2\xi-1$ (neglecting turning points), should be greater than or equal to $1+s$ so as to ensure interface-interface interactions; thus, it follows that $2\xi-1\geq 1+s$ or $s\leq 2\xi-2$ so that $s_u = 2\xi-2$ for a given ξ.

Therefore, including both planar and cross-planar correlations allows us to express the total $\Gamma = \Gamma_t$ as the sum of the two contributing terms $\Gamma_t = \Gamma_p + \Gamma_{cp}$ for "*p*" and "*cp*" contributions ($\Delta\omega_t$ can also be analyzed in a similar way). The total $\Gamma = \Gamma_t$ can be expressed as

$$\Gamma_t(K_{0\perp}) = \Gamma_0\sum_{m=-\infty}^{m_u}\sigma_m^{(t)} I_0(\beta_m)\, e^{(m\hbar\omega_B-\hbar^2K_{0\perp}^2/m_\perp)/\varepsilon_\lambda}, \quad (96)$$

with $\sigma_m^{(t)}(\xi) = \sigma_m(\xi)+\widetilde{\sigma}_m(\xi)$, where $\sigma_m(\xi)$ and $\widetilde{\sigma}_m(\xi)$ are defined in Eqs. (83) for "*p*" and (95) for "*cp*" contributions, respectively. We evaluate Γ_t in the manner used in the previous Sec. A, then Eq. (96) becomes

$$\frac{\Gamma_t(0)}{\Gamma'_0} = \zeta\sum_{m=1}^{\infty}\sigma_m^{(t)}(\xi)\, e^{-m\zeta/2\xi}. \quad (97)$$

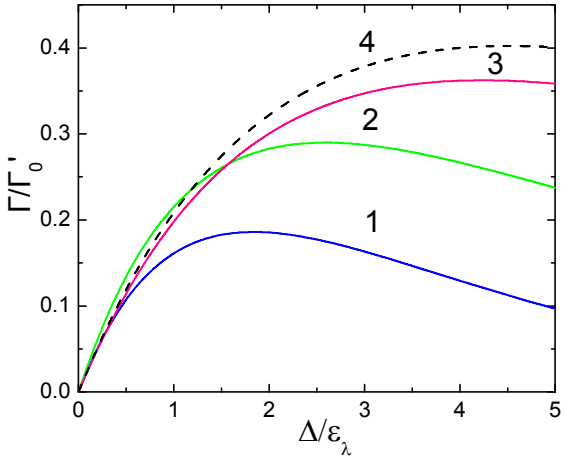

Fig. 4. Normalized relaxation rate $\Gamma(\zeta)/\Gamma'_0$ as a function of $\zeta = \Delta/\varepsilon_\lambda$ calculated for different values of $\xi = \Delta/2\hbar\omega_B$: $\xi = 1$ (*1*); $\xi = 2$ (*2*); $\xi = 3$ (*3*, *4*). The solid curves *1-3* take the planar correlations alone [Eq. (84)], while the dashed curve *4* takes the total, planar and cross-plane correlations [Eq. (97)].

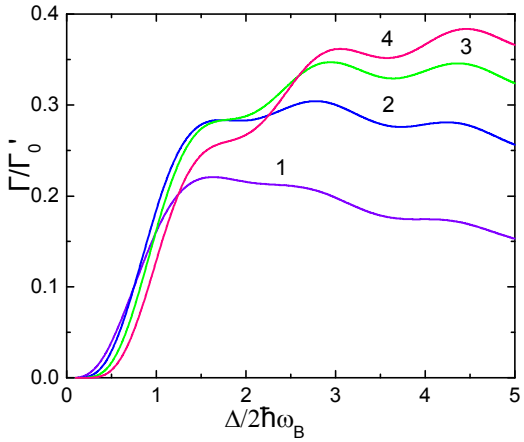

Fig. 5. Normalized relaxation rate $\Gamma(\xi)/\Gamma'_0$ as a function of $\xi = \Delta/2\hbar\omega_B$ calculated for different values of $\zeta = \Delta/\varepsilon_\lambda$ [Eq. (84)]: $\zeta = 1$ (*1*); $\zeta = 2$ (*2*); $\zeta = 3$ (*3*); $\zeta = 4$ (*4*).

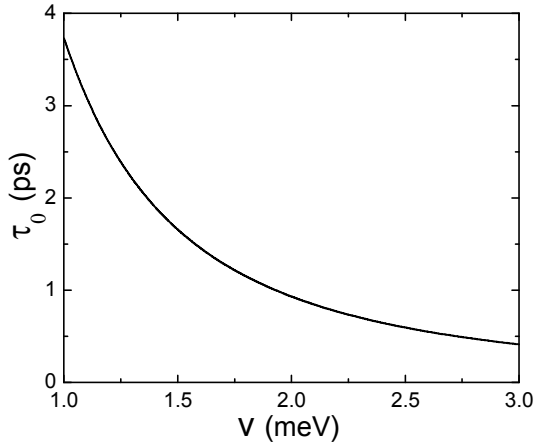

Fig. 6. The parameter $\tau_0 = 1/\Gamma'_0$ as a function of v ($\Delta = 36$ meV).

This equation has the form similar to Eq. (84) derived for planar correlations alone and shows the similar behavior as a function of ζ and ξ. In Eqs. (96) and (97), we can see that the term $\tilde{\sigma}_m$ in $\sigma_m^{(t)} = \sigma_m + \tilde{\sigma}_m$, which corresponds to cross-planar interference, is relatively small compared to the planar contribution, σ_m. As a numerical estimate of the contribution from cross-planar correlations in Eq. (97), we take $\xi = 3$ and $a/\delta = 1$, i.e., for $a = 10$ nm we take $\delta = 10$ nm. In this case, we obtain $\zeta_{max} \cong 4.9$ and $\Gamma(\zeta_{max})/\Gamma'_0 \cong 0.39$ (Fig. 4, dashed curve 4). The estimates show that, for the assumed values of the model parameters, the cross-planar contribution to the SE relaxation rate is about 8% as compared to the dominant independent planar term defined in Eq. (84).

It is worth noting that the developed methodology for evaluating the degradation effects from SE due to perturbing inhomogeneity in the SL is quite general and is not restricted to a one-dimensional (1D) quantum-well SL with the miniband dispersion as in Eq. (20). Recent progress in nanotechnology makes it possible to fabricate various kinds of SLs that are different from the usual periodically layered QW structures based on III-V compounds. [3-5] These examples include quantum-dot SLs of varying dimensionality (1D, 2D, and 3D SLs) [42, 43], graphene-based SLs [44-46], and natural SLs in SiC crystals [47], which, in particular, have been investigated for the practical realization of a Bloch-oscillation terahertz generator [48-52].

6. Summary

A theory for the spontaneous emission of Bloch oscillation radiation under the competing influences of microcavity environment and inhomogeneous interface scattering is presented. The external constant electric field strength is chosen so that the emitted radiation is in the terahertz spectral range; the quantum electromagnetic radiation field is described by the dominant TE_{10} rectangular microcavity waveguide mode in the Coulomb gauge. The instantaneous eigenstates of the Bloch Hamiltonian are used to describe the Bloch electron dynamics to all orders in the constant electric field, and the inhomogeneous electric field describing the interface inhomogeneities is treated in the scalar potential gauge. In general, it is shown that the spontaneous emission probability amplitude for the cavity-enhanced Bloch electron radiation becomes damped and frequency shifted due to the perturbing influence of the inhomogeneous electric field; the frequency shift is shown to be proportional to the second-order perturbation theory correction of the Hamiltonian for the perturbing inhomogeneity with respect to the Bloch instantaneous eigenstates, and the damping term is shown to be proportional to the square

of the off-diagonal transition matrix elements of the perturbing Hamiltonian with respect to the instantaneous eigenstates summed to the appropriate final states as determined in a golden-rule fashion. The general emission formulation with regard to competing influences lends itself to a heuristic relaxation approximation development; therefore, a simplified trend analysis was developed in order to explicitly characterize the degradation of cavity-enhanced spontaneous emission in a user friendly way; the results of this analysis clearly show that the degradation effects reflected in the probability amplitude as a result of the presence of interface inhomogeneities can be more than compensated for by the enhancements derived by microcavity-based confinement tuning. Finally, the general theoretical analysis is extended to the specific case where the inhomogeneous interface potential energy is represented by a comb of localized planar inhomogeneities of varying strength positioned at all the SL sites. The frequency shift and damping constant is discussed for this model problem as a methodology for going beyond the constant relaxation-time approximation. In this approach, the interface roughness effects were separated into those arising from independent planar and cross-correlated neighboring planar interfaces; it was estimated that the cross-correlated contribution to the spontaneous emission relaxation rate is relatively small, comprising less than roughly 10% of the total relaxation rate, compared to the independent planar contribution.

Although the special case of abrupt interface roughness treated in this work is time independent, the general treatment developed in the Appendix is applicable to the more general case of quantum spontaneous emission under the competing influence of a *general time-dependent perturbation*. This perturbation can also be made to depend on other degrees of freedom, so that the analysis provides a framework for examining the influence of phonon scattering on the spontaneous emission process; this will be the objective of a future study.

Appendix: Time-dependent double perturbation theory approach

The equation for the probability amplitudes $A_{\{n_{\mathbf{q},j}\}}(\mathbf{K},t)$ in Eq. (2) is given by

$$\frac{dA_{\{n_{\mathbf{q},j}\}}(\mathbf{K},t)}{dt}=\frac{1}{i\hbar}\sum_{\mathbf{K}'}\sum_{\{n'_{\mathbf{q},j}\}}A_{\{n'_{\mathbf{q},j}\}}(\mathbf{K}',t)\times$$
$$\langle\{n_{\mathbf{q},j}\},\psi_{n_0\mathbf{K}}(\mathbf{r},t)\,|\,(H_I+V)\,|\,\psi_{n_0\mathbf{K}'}(\mathbf{r},t),\{n'_{\mathbf{q},j}\}\rangle\times$$
$$\times\exp\left\{-\frac{i}{\hbar}\int_{t_0}^{t}[\varepsilon_{n_0}(\mathbf{k}'(t'))-\varepsilon_{n_0}(\mathbf{k}(t'))+\sum_{\mathbf{q},j}(n'_{\mathbf{q},j}-n_{\mathbf{q},j})\hbar\omega_q]\,dt'\right\}. \quad (A.1)$$

We assume that at initial time, t_0, the system is in one of the eigenstates of Hamiltonian H_0+H_r with wave function $|\psi_{n_0\mathbf{K}_0}(\mathbf{r}),\{n^0_{\mathbf{q},j}\}\rangle$, corresponding to the Bloch electron in a single band n_0 with the wave vector $\mathbf{K}_0$ and with the initial distribution of photon numbers in the radiation field $|\{n^0_{\mathbf{q},j}\}\rangle$. Substituting $A_{\{n_{\mathbf{q},j}\}}(\mathbf{K},t)=A^{(0)}_{\{n_{\mathbf{q},j}\}}(\mathbf{K},t)+A^{(1)}_{\{n_{\mathbf{q},j}\}}(\mathbf{K},t)+\ldots$ into Eq. (A.1), and taking into account the initial condition $A_{\{n_{n_{\mathbf{q},j}}\}}(\mathbf{K},t_0)=\{\delta_{n_{\mathbf{q},j}n^0_{\mathbf{q},j}}\}\delta_{\mathbf{K},\mathbf{K}_0}$, one obtains to the zeroth and first order in H_I for $A^{(0)}_{\{n_{\mathbf{q},j}\}}(\mathbf{K},t)$ and $A^{(1)}_{\{n_{\mathbf{q},j}\}}(\mathbf{K},t)$, respectively,

$$A^{(0)}_{\{n_{\mathbf{q},j}\}}(\mathbf{K},t)=\{\delta_{n_{\mathbf{q},j}n^0_{\mathbf{q},j}}\}\delta_{\mathbf{K},\mathbf{K}_0}, \quad (A.2)$$

and

$$\frac{dA^{(1)}_{\{n_{\mathbf{q},j}\}}(\mathbf{K},t)}{dt}-\frac{1}{i\hbar}\sum_{\mathbf{K}'}A^{(1)}_{\{n_{\mathbf{q},j}\}}(\mathbf{K}',t)V_{\mathbf{K},\mathbf{K}'}(t)\times$$
$$\times\exp\left\{-\frac{i}{\hbar}\int_{t_0}^{t}[\varepsilon_{n_0}(\mathbf{k}'(t'))-\varepsilon_{n_0}(\mathbf{k}(t'))]\,dt'\right\}=$$
$$=\frac{1}{i\hbar}\langle\{n_{\mathbf{q},j}\},\psi_{n_0\mathbf{K}}(\mathbf{r},t)\,|\,H_I\,|\,\psi_{n_0\mathbf{K}_0}(\mathbf{r},t),\{n^0_{\mathbf{q},j}\}\rangle\times$$
$$\times\exp\left\{-\frac{i}{\hbar}\int_{t_0}^{t}[\varepsilon_{n_0}(\mathbf{k}_0(t'))-\varepsilon_{n_0}(\mathbf{k}(t'))+\sum_{\mathbf{q},j}(n^0_{\mathbf{q},j}-n_{\mathbf{q},j})\hbar\omega_q]\,dt'\right\}; \quad (A.3)$$

this equation for $A^{(1)}_{\{n_{\mathbf{q},j}\}}(\mathbf{K},t)$ is good to first order in H_I and to all orders in V. Matrix elements for the perturbation operator H_I are given by

$$\langle\{n_{\mathbf{q}}\},\psi_{n_0\mathbf{K}}(\mathbf{r},t)\,|\,H_I\,|\,\psi_{n_0\mathbf{K}_0}(\mathbf{r},t),\{n^0_{\mathbf{q}}\}\rangle=$$
$$=\sqrt{\frac{\pi c\alpha}{\omega_c\varepsilon V_0}}\sum_{q'_z}\sum_{s=1,2}\frac{1}{[1+(q'_z/q_x)^2]^{1/4}}\nabla_{k_y}\varepsilon_{n_0}[\mathbf{k}(t)]\times$$
$$\times\left[\sqrt{n^0_{\mathbf{q}'}}(\delta_{n_{\mathbf{q}'},n^0_{\mathbf{q}'}-1};\{\delta_{n_{\mathbf{q}},n^0_{\mathbf{q}}}\})\,\delta_{\mathbf{K}_0,\mathbf{K}-\mathbf{q}'_s}+\right.$$
$$\left.+\sqrt{n^0_{\mathbf{q}'}+1}(\delta_{n_{\mathbf{q}},n^0_{\mathbf{q}'}+1};\{\delta_{n_{\mathbf{q}},n^0_{\mathbf{q}}}\})\delta_{\mathbf{K}_0,\mathbf{K}+\mathbf{q}'_s}\right]. \quad (A.4)$$

For brevity in using notation, Eq. (A.3) can be written as

$$\dot{A}_n(\mathbf{K},t)-\frac{1}{i\hbar}\sum_{\mathbf{K}'}f_{\mathbf{K}\mathbf{K}'}(t)A_n(\mathbf{K}',t)=\dot{A}^0_n(\mathbf{K},t), \quad (A.5)$$

with

$$f_{\mathbf{K}\mathbf{K}'}(t)=V_{\mathbf{K}\mathbf{K}'}(t)\exp\left\{-\frac{i}{\hbar}\int_{t_0}^{t}[\varepsilon_{n_0}(\mathbf{k}'(t'))-\varepsilon_{n_0}(\mathbf{k}(t'))]\,dt'\right\}, \quad (A.6)$$

where $V_{\mathbf{KK}'}(t) = (\psi_{n_0\mathbf{K}}(\mathbf{r},t), V\psi_{n_0\mathbf{K}'}(\mathbf{r},t))$, and

$$\dot{A}_n^0(\mathbf{K},t) = \frac{1}{i\hbar}\langle\{n_{\mathbf{q},j}\}, \psi_{n_0\mathbf{K}}(\mathbf{r},t) \mid H_I \mid \psi_{n_0\mathbf{K}_0}(\mathbf{r},t), \{n^0_{\mathbf{q},j}\}\rangle \times$$
$$\times \exp\left\{-\frac{i}{\hbar}\int_{t_0}^{t}[\varepsilon_{n_0}(\mathbf{k}_0(t')) - \varepsilon_{n_0}(\mathbf{k}(t')) + \sum_{\mathbf{q},j}(n^0_{\mathbf{q},j} - n_{\mathbf{q},j})\hbar\omega_q]dt'\right\}. \quad (A.7)$$

Again, it is emphasized that Eq. (A.5) is valid to the first order in H_I and to all orders in V . Also to simplify notations, we designated $A^{(1)}_{\{n_{\mathbf{q},j}\}}(\mathbf{K},t) \equiv A_n(\mathbf{K},t)$. Then, separating terms with diagonal and off-diagonal matrix elements $f_{\mathbf{K},\mathbf{K}'}(t)$ in Eq . (A.5) so that

$$\dot{A}_n(\mathbf{K},t) - \frac{1}{i\hbar}f_{\mathbf{KK}}(t)A_n(\mathbf{K},t) -$$
$$-\frac{1}{i\hbar}\sum_{\mathbf{K}'\neq\mathbf{K}} f_{\mathbf{KK}'}(t)A_n(\mathbf{K}',t) = \dot{A}_n^0(\mathbf{K},t) , \quad (A.8)$$

the equation for $A_n(\mathbf{K}',t)$ in the third term on the left-hand side of (A.8) can be written as

$$\dot{A}_n(\mathbf{K}',t) - \frac{1}{i\hbar}f_{\mathbf{K}'\mathbf{K}}(t)A_n(\mathbf{K},t) -$$
$$-\frac{1}{i\hbar}\sum_{\mathbf{K}''\neq\mathbf{K}} f_{\mathbf{K}'\mathbf{K}''}(t)A_n(\mathbf{K}'',t) = \dot{A}_n^0(\mathbf{K}',t). \quad (A.9)$$

Following to the Wigner–Weisskopf-like approximation, we ignore the third term on the right-hand side of (A.9); then, after integration on time, we find

$$A_n(\mathbf{K}',t) = \frac{1}{i\hbar}\int_{t_0}^{t} dt' f_{\mathbf{K}'\mathbf{K}}(t')A_n(\mathbf{K},t') + A_n^0(\mathbf{K}',t), \quad (A.10)$$

where we have taken into account that $A_n(\mathbf{K}',t_0) = \delta_{\mathbf{K}',\mathbf{K}_0}$, i.e., is equal to zero for $\mathbf{K}' \neq \mathbf{K}_0$, and

$$A_n^0(\mathbf{K},t) = \int_{t_0}^{t}\dot{A}_n^0(\mathbf{K},t')dt'. \quad (A.11)$$

Thus, by making use of (A.10) in Eq. (A.8), we obtain the latter equation in the form

$$\dot{A}_n(\mathbf{K},t) - \frac{1}{i\hbar}f_{\mathbf{KK}}(t)A_n(\mathbf{K},t) +$$
$$+\frac{1}{\hbar^2}\sum_{\mathbf{K}'\neq\mathbf{K}} f_{\mathbf{KK}'}(t)\int_{t_0}^{t} dt' f^*_{\mathbf{KK}'}(t')A_n(\mathbf{K},t') =$$
$$= \dot{A}_n^0(\mathbf{K},t) + \frac{1}{i\hbar}\sum_{\mathbf{K}'\neq\mathbf{K}} f_{\mathbf{KK}'}(t)A_n^0(\mathbf{K}',t). \quad (A.12)$$

Here, the solution to Eq. (A.12) represents an early-time, first-order perturbation theory solution for H_I , and a long-time, Wigner–Weisskopf-like perturbation solution for V in this double perturbation theory approach.

References

1. E.M. Purcell, Spontaneous emission probabilities at radio frequencies // *Phys. Rev.* **69** (11-12), p. 681 (1946).
2. E. Yablonovitch, Inhibited spontaneous emission in solid-state physics and electronics // *Phys. Rev. Lett.* **58**(20), p. 2059-2062 (1987).
3. L. Esaki and R. Tsu, Superlattice and negative differential conductivity in semiconductors // *IBM J. Res. Dev*. **14**(1), p. 61-65 (1970).
4. R. Tsu, Applying the insight into superlattices and quantum wells for nanostructures: Low-dimensional structures and devices // *Microelectron. J*. **38**(10-11), p. 959-1012 (2007).
5. R. Tsu, Superlattices: problems and new opportunities, nanosolids // *Nano. Res. Lett*. **6**(1), p. 127(10), (2011).
6. H.G. Roskos, Coherent emission of electromagnetic pulses from Bloch oscillations in semiconductor superlattices, *Advances in Solid State Physics*. Vol. 34, p. 297. Edited by R. Helbig, Berlin Heidelberg, Springer, 1994.
7. K. Leo, Interband optical investigation of Bloch oscillations in semiconductor superlattices // *Semicond. Sci. Technol*. **13**(3), p. 249-263 (1998).
8. E.E. Mendez and G. Bastard, Wannier-Stark ladders and Bloch oscillations in superlattices // *Phys. Today,* **46**(6), p. 34-42 (1993).
9. T. Dekorsy, R. Ott, H. Kurz, and K. Köhler, Bloch oscillations at room temperature // *Phys. Rev. B*, **51**(23), p. 17275-17278(R) (1995).
10. P. Robrish, J. Xu, S. Kobayashi, P.G. Savvidis, B. Kolasa, G. Lee, D. Mars, and S.J. Allen, Loss and gain in Bloch oscillating super-lattices: THz Stark ladder spectroscopy // *Physica E*, **32**(1-2), p. 325-328 (2006);
11. P.G. Savvidis, B. Kolasa, G. Lee, and S.J. Allen, Resonant crossover of terahertz loss to the gain of Bloch oscillating InAs/AlSb superlattice // *Phys. Rev. Lett*. **92**(19), 196802(4) (2004).
12. T. Hyart, N.V. Alexeeva, J. Mattas, and K.N. Alekseev, Terahertz Bloch oscillator with a modulated bias // *Phys. Rev. Lett.* **102**(14), 140405(4), (2009).
13. K.F. Renk, *Basics of Laser Physics*. Springer-Verlag, Berlin, 2012. Superlattice Bloch laser: A Challenge, Part V, Semiconductor lasers, Ch. 32, p. 539.
14. V.N. Sokolov, G.J. Iafrate, and J.B. Krieger, Microcavity enhancement of spontaneous emission for Bloch oscillations // *Phys. Rev. B*, **75**(4), 045330(6), (2007).
15. V.N. Sokolov and G.J. Iafrate, Spontaneous emission of Bloch oscillation radiation in the terahertz regime, Chap. 6, in: *Handbook of Nanoscience, Engineering and Technology*. 3 ed., Eds. W.A. Goddard *et al.*, CRC Press, New York, 2011, p. 67-124.

16. V.N. Sokolov, L. Zhou, G.J. Iafrate, and J.B. Krieger, Spontaneous emission of Bloch oscillation radiation from a single energy band // *Phys. Rev. B*, **73**(20), 205304(11), (2006).
17. T. Unuma, N. Sekine, and K. Hirakawa, Dephasing of Bloch oscillating electrons in GaAs-based superlattices due to interface roughness scattering // *Appl. Phys. Lett*. **89**(16), 161913(3), (2006).
18. Y.T. Chiu, Y. Dikmelik, P.Q. Liu, N.L. Aung, J.B. Khurgin, and C.F. Gmachl, Importance of interface roughness induced intersubband scattering in mid-ifrared quantum cascade lasers // *Appl. Phys. Lett*. **101**(17), 171117(4), (2012).
19. M.P. Semtsiv, Y. Flores, M. Chashnikova, G. Monastyrskyi, and W.T. Masselink, Low-threshold intersubband laser on interface-scattering-rate engineering // *Appl. Phys. Lett*. **100**(16), 163502(3), (2012).
20. M.P. Telenkov and Y.A. Mityagin, A microscopic model of sequential resonant tunneling transport through weakly coupled superlattices // *Sov. Phys. JETP,* **99**(3), p. 620-632 (2004) [*Zh. Eksp. Teor. Fiz*. **126**(3), p. 712-726 (2004), in Russian].
21. V.N. Sokolov and G.J. Iafrate, Spontaneous emission of Bloch oscillation radiation under the competing influences of microcavity enhancement and inhomogeneous interface degradation // *J. Appl. Phys.* **115** (5), 054307 (12), (2014).
22. J.B. Krieger and G.J. Iafrate, Time evolution of Bloch electrons in a homogeneous electric field // *Phys. Rev. B*, **33**(8), p. 5494-5500 (1986).
23. G.J. Iafrate and J.B. Krieger, Quantum transport for Bloch electrons in inhomogeneous elecric fields // *Phys. Rev*. **40**(9), p. 6144-6148 (1989).
24. D. Marcuse, *Principles of Quantum Electronics*. Academic, New York, 1980, p. 426.
25. N. Marcuvitz, *Waveguide Handbook*. Peregrinus, London, 1993.
26. W.H. Louisell, *Quantum Statistical Properties of Radiation*. Wiley and Sons, New York, 1973, p. 57.
27. J. He and G.J. Iafrate, Multiband theory of Bloch-electron dynamics in a homogeneous electric field // *Phys. Rev. B,* **50**(11), p. 7553-7566 (1994).
28. E. Merzbacher, *Quantum Mechanics*. Wiley and Sons, New York, 1970, p. 484-485; Ref. [26], p. 288.
29. C. Kittel, *Quantum Theory of Solids*. Wiley and Sons, New York, 1963, p. 185, Eq. (49) therein.
30. I. Dharssi and P.N. Butcher, Interface roughness scattering in a superlattice // *J. Phys.*: *Condens. Matter,* **2**(20), p. 4629-4635 (1990).
31. G. Fishman and D. Calecki, Surface-induced resistivity of ultrathin metalic films: A limit law // *Phys. Rev. Lett*. **62**(11), p. 1302-1305 (1989).
32. G. Kastrinakis, Interface roughness and planar doping in superlattices: weak localization effects // *Solid State Communs*. **125**(10), p. 533-536 (2003).
33. R.E. Prange and T.-W. Nee, Quantum spectroscopy of the low-field oscillations in the surface impedance // *Phys. Rev*. **168**(3), p. 779-786 (1968).
34. S.M. Goodnick, D.K. Ferry, C.W. Wilmsen, Z. Liliental, D. Fathy, and O.L. Krivanek, Surface roughness at the Si(100)-SiO_2 interface // *Phys. Rev. B*, **32**(12), p. 8171-8186 (1985).
35. G.N. Watson, *A Treatise on the Theory of Bessel Functions*. Cambridge, University Press, 1944, p. 22.
36. D.K. Ferry, *Semiconductor Transport*. Taylor and Francis, New York, 2000, p. 87.
37. J. He and G.J. Iafrate, The effects of band structure and electric field on resonant tunneling dynamics, in *Quantum Transport in Ultrasmall Devices*. NATO ASI series, Series B, Theory; Physics, Vol. 342, Eds. D.K. Ferry *et al.*, Plenum, New York, 1995, p. 281.
38. M.O. Scully and M.S. Zubairy, *Quantum Optics*. Cambridge, 1997, p. 282-285.
39. P.M. Morse and H. Feshbach, *Methods of Theoretical Physics*. McGraw-Hill, New York, 1953, part 1, p. 467.
40. V. Holý and T. Baumbach, Nonspecular x-ray reflection from rough multilayers // *Phys. Rev. B*, **49**(15), p. 10668-10676 (1994).
41. G. Palasantzas and J.Th.M. De Hosson, Effect of roughness on the conductivity of semiconducting thin films/quantum wells with double rough boundaries // *J. Appl. Phys*. **93**(1), p. 320-324 (2003).
42. I.A. Dmitriev and R.A. Suris, Dephasing of Bloch oscillations in quantum dot superlattices: A general approach // *Semiconductors*, **36**(12), p. 1364-1374 (2002) [*Fizika Tekhnika Poluprovodn.* **36**(12), p. 1449-1459 (2002), in Russian].
43. V.G. Talalaev, G.E. Cirlin, A.A. Tonkikh, N.D. Zakharov, P. Werner, U. Gösele, J.W. Tomm, and T. Elsaesser, Miniband-related 1.4-1.8 μm luminiscence of Ge/Si quantum dot superlattices // *Nano. Res. Lett*. **1**, p. 137-153 (2006).
44. C.-H. Park, L. Yang, Y.-W. Son, M.L. Cohen, and S.G. Louie, Anisotropic behaviours of massless Dirac fermions in graphene under periodic potentials // *Nature Phys*. **4**, p. 213-217 (2008).
45. H. Sevincli, M. Topsakal, and S. Ciraci, Super-lattice structure of graphene-based armchair nano-ribbons // *Phys. Rev. B*, **78**(24), 245402(8), (2008).
46. D. Dragoman and M. Dragoman, Terahertz Bloch oscillations in periodic graphene structures // *Appl. Phys. Lett*. **93**(10), p. 103105(3) (2008).
47. V.I. Sankin, Wannier-Stark localization in the natural superlattice of silicon carbide polytypes // *Semiconductors*, **36**(7), p. 717-739 (2002) [*Fizika Tekhnika Poluprovodn.* **36**(7), p. 769-793 (2002), in Russian].
48. R.A. Suris and I.A. Dmitriev, Bloch oscillations in quantum dot superlattices // *Phys. Usp*. **46**(7), p. 745-751 (2003) [*Uspekhi Fiz. Nauk*, **173**(7), p. 769-76 (2003), in Russian].

49. Yu.A. Romanov and Yu.Yu. Romanova, Bloch oscillations in superlattices: The problem of a terahertz oscillator // *Semiconductors*, **39**(1), p. 147-155 (2005) [*Fizika Tekhnika Poluprovodn.* **39**(1), p. 162-170 (2005), in Russian].
50. S.K. Lyo, Bloch oscillations and nonlinear transport in a one-dimensional semiconductor superlattice // *Phys. Rev. B*, **77**(19), 195306(8), (2008).
51. Yu.A. Romanov, J.Yu. Romanova, and L.G. Mourokh, Electron Bloch oscillations and electromagnetic transparency of semiconductor superlattices in multi-frequency electric fields // *Phys. Rev. B*, **79**(24), 245320(18), (2009).
52. V.I. Sankin, A.V. Andrianov, A.O. Zakhar'in, and A.G. Petrov, Terahertz electroluminiscence from 6H-SiC structures with natural superlattice // *Appl. Phys. Lett*. **100**(11), 111109(4), (2012).